Preliminary analysis of wind profiles measured with an MFAS-SODAR at Split Airport in the period June-November 2022

Jakić, Jure

Master's thesis / Diplomski rad

2024

Degree Grantor / Ustanova koja je dodijelila akademski / stručni stupanj: **University of Split, Faculty of Science / Sveučilište u Splitu, Prirodoslovno-matematički fakultet**

Permanent link / Trajna poveznica: https://urn.nsk.hr/urn:nbn:hr:166:911924

Rights / Prava: In copyright/Zaštićeno autorskim pravom.

Download date / Datum preuzimanja: **2025-02-28**

zir.nsk.hr   UNIVERSITY OF SPLIT   dabar

DIGITALNI AKADEMSKI ARHIVI I REPOZITORIJI

Sveučilište u Splitu

Prirodoslovno-matematički fakultet

Preliminary analysis of wind profiles measured with an MFAS-SODAR at Split Airport in the period June-November 2022

Master thesis

Jure Jakić

Split, March 2024.

Preliminarna analiza profila vjetra mjerenih MFAS Sodarom u Zračnoj luci Split tijekom razdoblja lipanj-studeni 2022

Jure Jakić

Sveučilišni diplomski studij Fizika, smjer Fizika okoliša

Sažetak:

MFAS SODAR postavljen je u Zračnoj luci Split u prosincu 2022. Analizirano je šest mjeseci mjerenja, počevši od lipnja do studenog 2022. godine. Tijekom tog razdoblja vremenski korak je bio 20 minuta, što za rezultat ima 20- minutni prosjekom horizontalnog i vertikalnog vjetra na visinama od 30 metara do najviše 400 metara, pri čemu je vertikalni razmak 10 metara. Mjerenja su obavljena u periodu lipanj-studeni 2022. Prevladavali su zmorac i burin koji su dodatno analizirani. Izračunati su dnevni vertikalni profili zmorca i burina. Preliminarna analiza pokazala je da su tijekom dnevnih sati horizontalni vjetrovi u prvih 400 metara bili dosta ujednačeni i zadržali svoj smjer, no dobijali na brzini s porastom visine. Sinoptički uvijeti za pojavu prethodno navedenih vjetrova su izdvojeni korištenjem skupa podataka ERA5 reanalize.

<div style="border:1px solid">

Basic documentation card

</div>

University of Split
Faculty of Science   Master thesis
Department of Physics
Ruđera Boškovića 33, 21000 Split, Croatia

Preliminary analysis of wind profiles measured with an MFAS-SODAR at Split Airport in the period June-November 2022

Jure Jakić

Physics, specialization in Environmental Physics

Abstract:
The Scintec Acoustic Wind Profiler SODAR MFAS was installed at Split Airport (on the Adriatic coast, Croatia) in December 2022. Six months of measurements, from June to November 2022, were analysed: during this period. The time step of the measurements was set to 20 minutes, resulting in 20-minute averages of horizontal and vertical wind at heights ranging from 30 m to a maximum of 400 m, with a 10-m vertical interval. The land and sea breezes were the predominant winds, and were further analysed. The mean daily vertical profile of the land and sea breezes was estimated. Preliminary analyses indicate that during the daytime hours, the horizontal winds were fairly uniform in the first 400 m and maintained their direction but gained some speed with height. On the other hand, a reversal of circulation was frequently observed during the nighttime hours. The synoptic conditions favourable for the occurrence of land and sea breezes were extracted using the ERA5 Global Reanalysis dataset.

Contents

1 Introduction

The area of the Split airport is characterized by many local winds (bora wind, sirocco, land breeze, sea breeze and so on. To understand their characteristics, an MFAS sound detection and ranging device (SODAR) was installed at the Split airport (Figure 1). By sending soundwaves into the atmosphere and receiving and analysing the reflected signal with a Doppler shift, MFAS SODAR data provide us with horizontal and vertical components of wind, measured from near surface to a maximum height (at most up to 1000 m).

MATLAB was used to analyse data measured by MFAS SODAR. Main goal of my research was to determine dominant winds at the Split airport during the investigated period, in particular land and sea breezes, and to determine prevailing synoptic situations during occurrence of land and sea breezes using the ERA5 reanalysis data (Hershbach et al., 2020).

Figure 1 MFAS SODAR at the Split airport.

2 MFAS SODAR

The Scintec MFAS is a compact acoustic profiler for the measurement of wind and turbulence up to 1000 m above the ground. The operation is based on the reflection of acoustic pulses at temperature inhomogeneities in the air and a subsequent doppler analysis.

The MFAS system consist of the following units:

- o   Acoustic antenna,
- o   Signal Processing Unit,
- o   Acoustic enclosure,
- o   Power supply,
- o   Antenna heating power supply.

Scintec Flat Array SODAR operate with an active acoustic antenna (of 0.72 m base length and 32 kg weight). This means that the antenna does not only house the transducers and switches, but also contains audio power drivers for emission and audio preamplifiers for reception mode. As emission elements, highly efficient transducers are used. The same elements reconvert the received sound waves into electric signals. The acoustic antenna is powered by an external power supply (AC converter or battery) of ±12 VDC. [1]

The Signal Processing Unit operates as a slave processor following the instructions from the terminal PC. The Signal Processing Unit performs the following functions:

- o   Generation of the acoustic emission signals for all 8 rows or columns.
- o   Control of the gain settings of the acoustic antenna.
- o   Control of the direction modes (vertical, East-West, North-South) of the acoustic antenna.
- o   Control of the operation mode (emission/reception) of the acoustic antenna.
- o   Power management of the acoustic antenna.
- o   Analog processing of the received signals.
- o   Analog-to-digital conversion of the return signals from the acoustic antenna.
- o   Combining the return signals of the rows and columns of the acoustic antenna with appropriate phase shifts.

- o Calculation of the Fourier transforms.

- o Temporal averaging of spectra.

- o Serial transmission of spectra to terminal PC.

The Signal Processing Unit is connected to the acoustic antenna. All transducers are directly controlled by the Signal Processing Unit. For this purpose, two signal cables are needed. The Signal Processing Unit is supplied with electrical power from the acoustic antenna. [1] The large enclosure consists of 16 panels and is placed around the SODAR antenna. The support stand is used to elevate the SODAR antenna from the ground. The attached electronic compartment is used to store the outdoor units and the enclosure is directly attached to the support stand. [1]

The power supply is an AC adapter which provides the required ±12 VDC output power for the acoustic antenna and Processing Unit. Two LEDs signalize the correct DC voltages. The following AC line voltage versions are available:

- o 110 - 120 VAC, 50/60 Hz,

- o 220 - 240 VAC, 50/60 Hz.

The additional power supply is an AC adapter which provides the required 24 VAC output power for the MFAS acoustic antenna heating. [1]

3 Characteristic winds

Split airport is located at the coast of Kaštela Bay, a 14,8 x 6,6 km large bay, located in the Adriatic Sea at the pedestal 779 m high Kozjak mountain (Figure 2). Winds characteristic for this area are: sirocco/jugo, bora (cro. bura), mistral (cro. maestral), tramontana, lebić and many others. Ones that appear the most are sirocco/jugo, bora, mistral, oštro, lebić or garbin, pulenat and land and sea breezes. [2] The Sirocco wind, originating from the Sahara Desert in Northern Africa, is a hot, dry, and often dusty wind that blows across the Mediterranean Sea into southern/southeast Europe. Known for its warmth and aridity, it significantly influences weather conditions in these regions, typically bringing high temperatures, reduced visibility due to dust and sand particles, and occasionally contributing to wildfires. The Sirocco wind is most prevalent during the spring and summer months when temperature differentials between the Sahara Desert and the Mediterranean Sea are most pronounced. Despite its adverse effects, the Sirocco wind also plays a role in shaping local ecosystems and can sometimes bring beneficial rain to certain areas. Nevertheless, Jurčec et al. (1996) claim that jugo is not generally sirocco, although jugo of gale force may have synoptic characteristics of sirocco. [3]
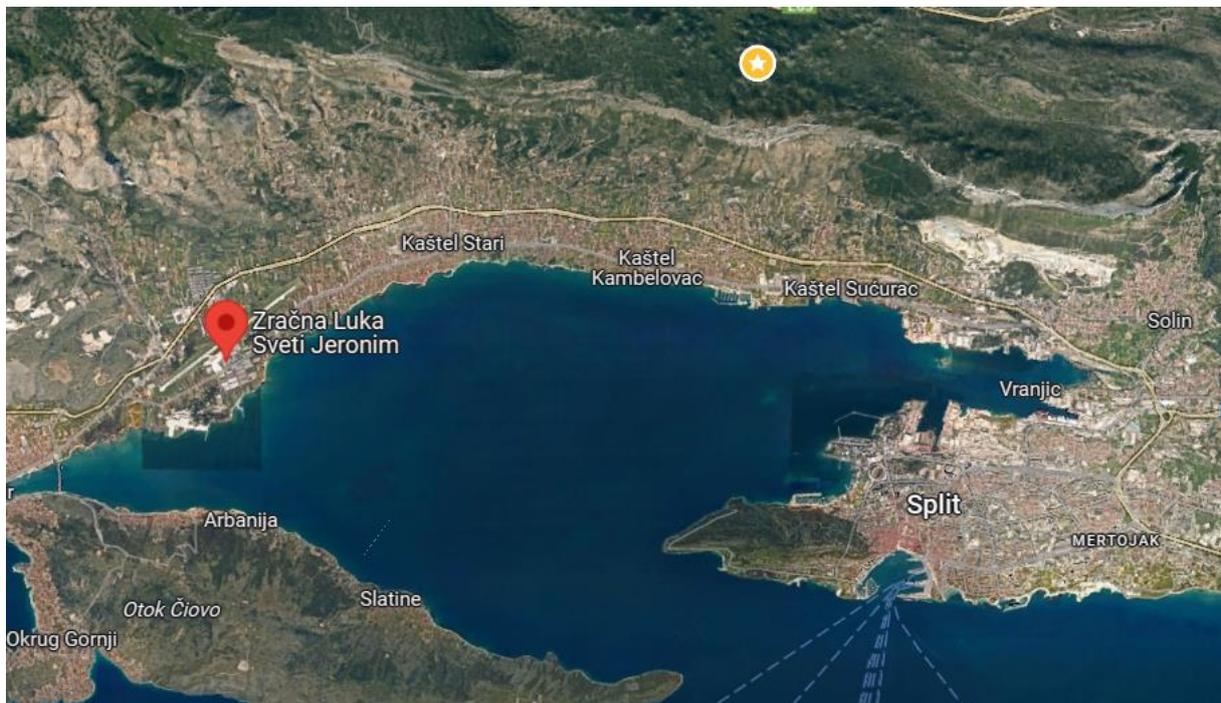
Figure 2 Kaštela Bay; yellow star indicates Kozjak mountain and red pin indicates Split airport location.

The other common wind at the Adriatic Sea is bora. If the fast-moving cold air upstream is deeper than the ridge height H (Figure 3), then very fast (hurricane force) cold winds can descend the lee side. This phenomenon is called bora. The winds accelerate in the constriction between mountain and the overlying inversion, and pressure drops according to the Venturi effect. The lower pressure upsets hydrostatic balance and draws the cold air layer downward, causing fast winds to flow over the slope.

Figure 3 Cold Bora winds, during synoptic weather patterns where strong winds are forced toward the ridge from upstream. Plot was downloaded directly from WindyApp textbook.

Bora is a vigorous, temporally and spatially transient, usually dry downslope wind. Mean bora wind velocities rarely exceed 30 m/s, while one of bora main characteristics is gustiness when the wind velocity may reach up to five times the mean velocity. Bora significantly influences vehicles and structures, especially in locations where it occurs rather frequently, like the town of Senj, Croatia, where Bora blows on average 177 days a year. While jugo is usually less severe than bora it can still reach locally more than 35 m/s and it can be very dangerous. [4]

Both jugo and bora appear due to larger synoptic systems and strong pressure gradients over the Adriatic Sea. On the contrary, during warm days with weak synoptic pressure gradients over the Adriatic, two local winds appear: sea breeze and land breeze. [4] Sea breeze is a shallow cool wind that blows onshore (from sea to land) during daytime (Figure 4). It occurs in large-scale high-pressure regions of weak or calm geostrophic wind under mostly clear skies. Similar flows called lake breezes form along lake shorelines, and inland sea breezes form along boundaries between adjacent land regions with different land-use characteristics (e.g., irrigated fields of crops adjacent to drier land with less vegetation). The sea breeze is caused by a 5 °C or greater temperature difference between the sun-heated warm land and the cooler water. It is a surface manifestation of a thermally driven mesoscale circulation called the sea-breeze circulation, which also includes a return flow aloft from land to sea. [4] During the night, after sunset, the land cools down more quickly than the sea because it has a lower heat capacity. The circulation of land and sea breezes is determined by the difference in horizontal pressure gradient at higher altitudes. Aloft, the horizontal pressure gradient ($\Delta P / \Delta y$) between warm and cold air columns generates horizontal winds from areas of high pressure to low pressure. Because winds denote the movement of air parcels, this implies that molecules leave regions with high pressure perturbations and accumulate in low-pressure areas. Specifically, they exit the warm column and enter the cold column. Therefore, the cold column now contains more molecules (i.e., more mass), leading to higher surface pressure (H) in the cold column. Conversely, the loss of mass from the warm column results in lower surface pressure (L), creating what is known as a thermal low. This phenomenon results in high pressure near the surface in the cold air, driving winds toward the low pressure in the warm air. Aloft, the high pressure perturbation in the warm air generate winds toward the low pressure perturbation in the cold air. This thermal circulation ensures that each column gains as many air molecules as it loses, maintaining mass equilibrium within the system.
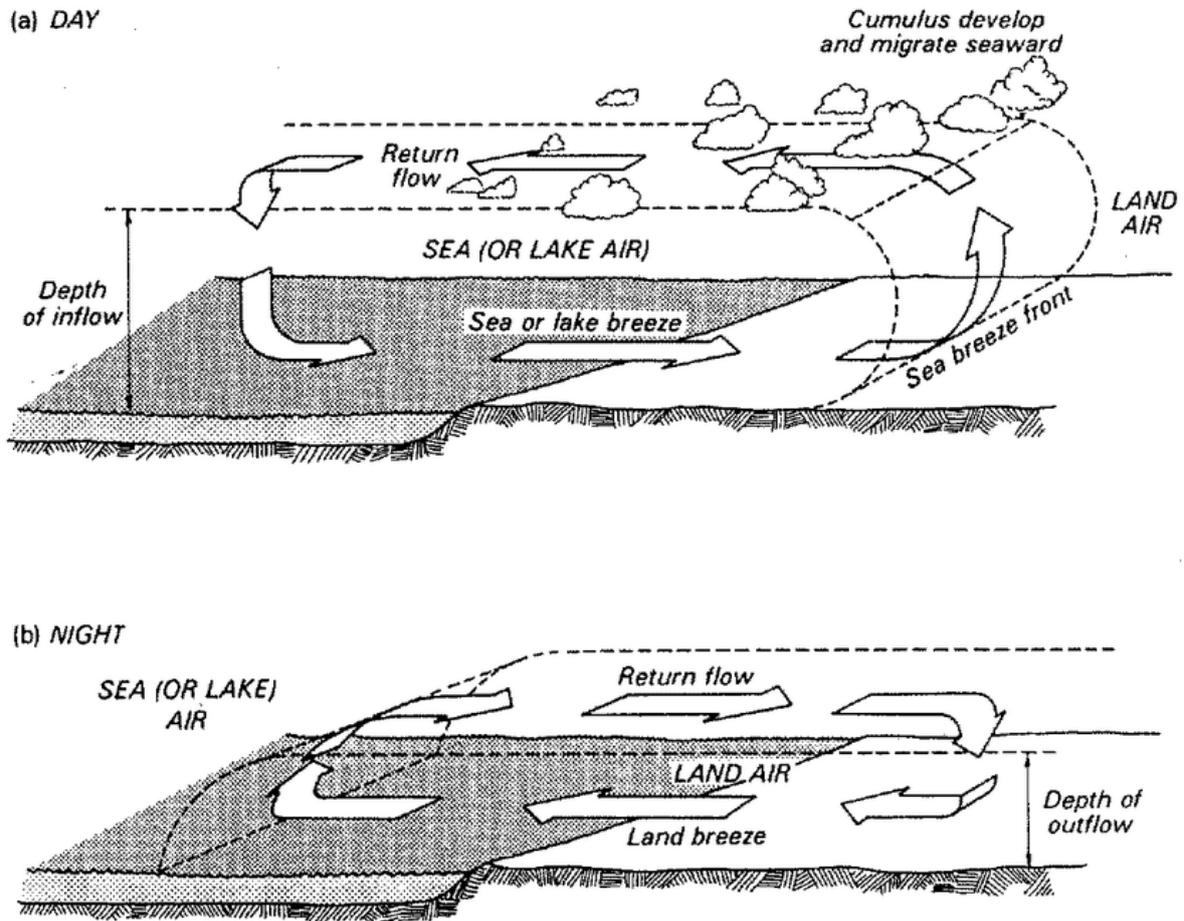
Figure 4 Vertical cross section through a sea-breeze circulation (from Oke, 1987, p. 168, fig. 5.6).

At the end of the day, sea-breeze circulation dissipates, and a weaker, reverse circulation called land-breeze forms in response to the nighttime cooling of the land surface relative to the sea. Sometimes, the now-disconnected sea-breeze front from late afternoon continues to advance farther inland during the night as a bore (the front of dense fluid advancing under less-dense fluid; also described as a propagating solitary wave with characteristics like the hydraulic jump). [2] Near 22:00 local time, the cool pool phenomenon caused by the effect of the sea breeze plus nocturnal cooling is about to form. The central portion of the pool is roughly parallel to the shoreline about 20 km inland. At the same time, a temperature inversion and

occasionally fog appear over land. The nearly barotropic field is prevailing over the area. By this time, the sea breeze is almost gone. Surface wind is nearly calm on land. [5] Despite the fact that sea/land breezes are quite frequent along the northern Adriatic Croatian coast (between 40%–65% of days) during the warm part of the year, it is still not a very well examined phenomenon. There are only a few studies, which describe the average 24-hourly cycle of sea/land breezes. Firstly, Orlić et al. (1988) demonstrated by applying a rotary spectra analysis the clockwise and anticlockwise rotary motions at three meteorological stations (Rijeka, Senj, Pula-Airport) in the northern Adriatic. Then, Lukišić (1989) described the main characteristics of diurnal winds at the Senj station. These studies revealed an anticlockwise rotation (ACR) at the Senj station, which is unusual for the Northern hemisphere. At the Rijeka and Pula-Airport stations, Coriolis-induced veering (clockwise rotation (CR)) was found. [6]

The aim of this research was to determine prevailing winds at the Split airport during June – November 2022, and to analyse in more detail land and sea breezes. Two data sets are used:

- o   measurements collected by MFAS SODAR installed at the airport and
- o   ERA5 hourly data set.

In situ measurements used for analysis cover a period from 20 June 2022 to 31 November 2022 (Figure 5). Because of the different technical difficulties data was not available or not analysed for the entire period but just for the dates shown. Of the possible 164 days, we had 111 days complete for analysis, or more precisely ≈67.7%.
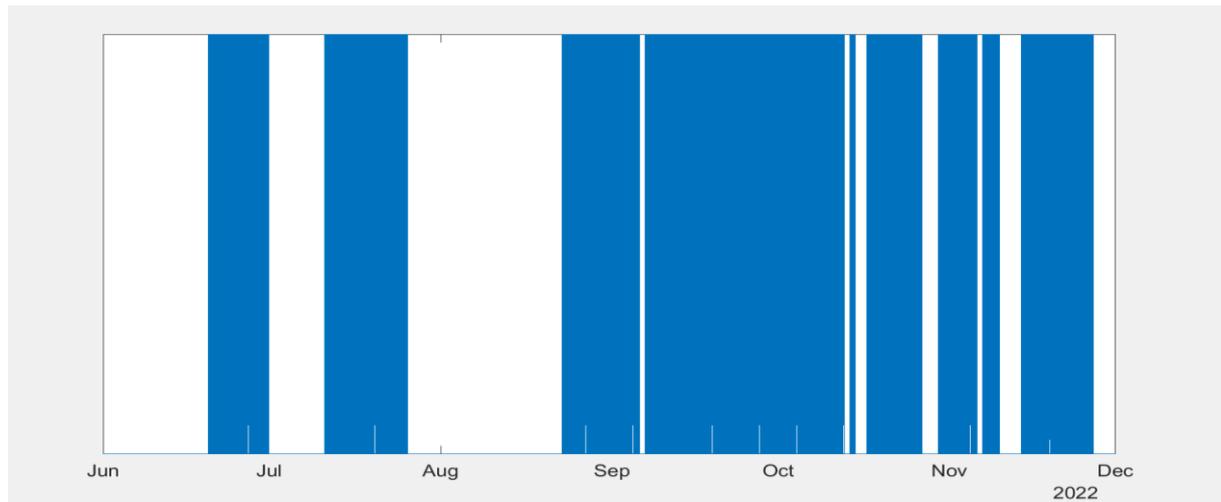
Figure 5 Availability of the data. Dates for which data were available are indicated in blue.

To determine typical synoptic conditions during days with sea breeze, ERA5 reanalyses data were used. Data has latitude-longitude grid resolution of 0.25 degrees. The data set that is analysed contains 26 days when land and sea breeze occurred at the Split airport (according to the MFAS data). The ERA5 variables that were analysed are: mean sea level pressure (MSLP), geopotential (at 500 hPa), 10 m u-component of the wind, 10 m v-component of the wind and the temperature; all at 15:00 CET and 23:00 CET of days with sea breeze, as well as monthly average values (for June to November) of the same variables. [6]

4 Results

4.1 Data availability

One of the issues while dealing with data was to determine the availability of the data vs. measurement heights. From Figure 6 one can notice that as the height increases, the percentage of available data decreases. Up to the height of approximately 120 m, 85 % of data is available, while at the height of 370 m less than 50% of data is available.
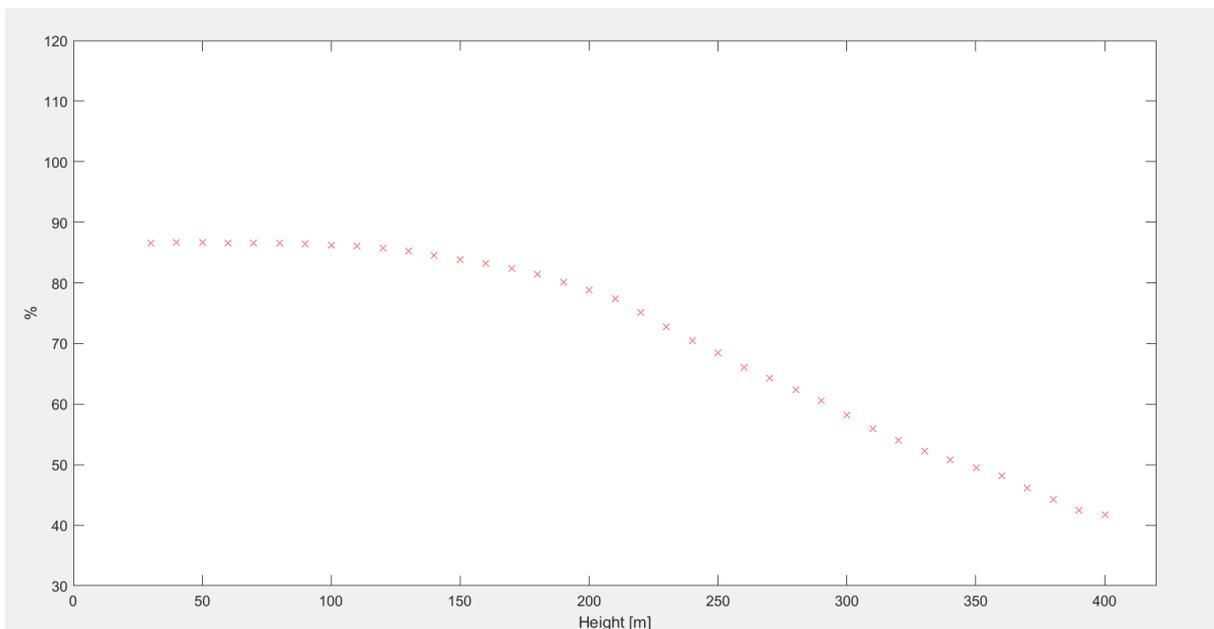
Figure 6 Availability (%) of data with respect to height during days marked with blue in Figure 4.

I also checked data availability as a function of hour and height (Figure 7). Up to 90% of measurements are available from 14:20 – 16:40 CET at 30-60 m height, while simultaneously, less than 20% of measurements are available for the same time interval, for altitudes above 330 m. In general, at heights above 200 m, availability of measurements declines during daylight hours, with minimum availability around 14-16 CET. Several factors can cause a lack of data or limitations in SODAR measurements in the atmosphere:

1) Weather Conditions: Adverse weather conditions such as heavy rain, fog, or snow can obstruct the SODAR signals, making it difficult for the instrument to obtain accurate measurements.

2) Obstructions: Buildings, trees, mountains, or other obstacles in the vicinity of the SODAR can interfere with the signals, leading to incomplete or distorted data.

3) Complex Atmospheric Conditions: Inhomogeneous or complex atmospheric conditions, such as strong vertical wind shear or rapidly changing temperature profiles, can challenge the SODAR's ability to provide continuous and reliable data.

Obviously, (1) and (2) cannot explain lack of data during certain hours of a warmer and drier period of year [2]. Thus, the observed decrease of availability of data must be to (3) inhomogeneous or complex atmospheric conditions which might be related to a temperature inversion at height of 200 m and above; or to change in wind direction at these heights.
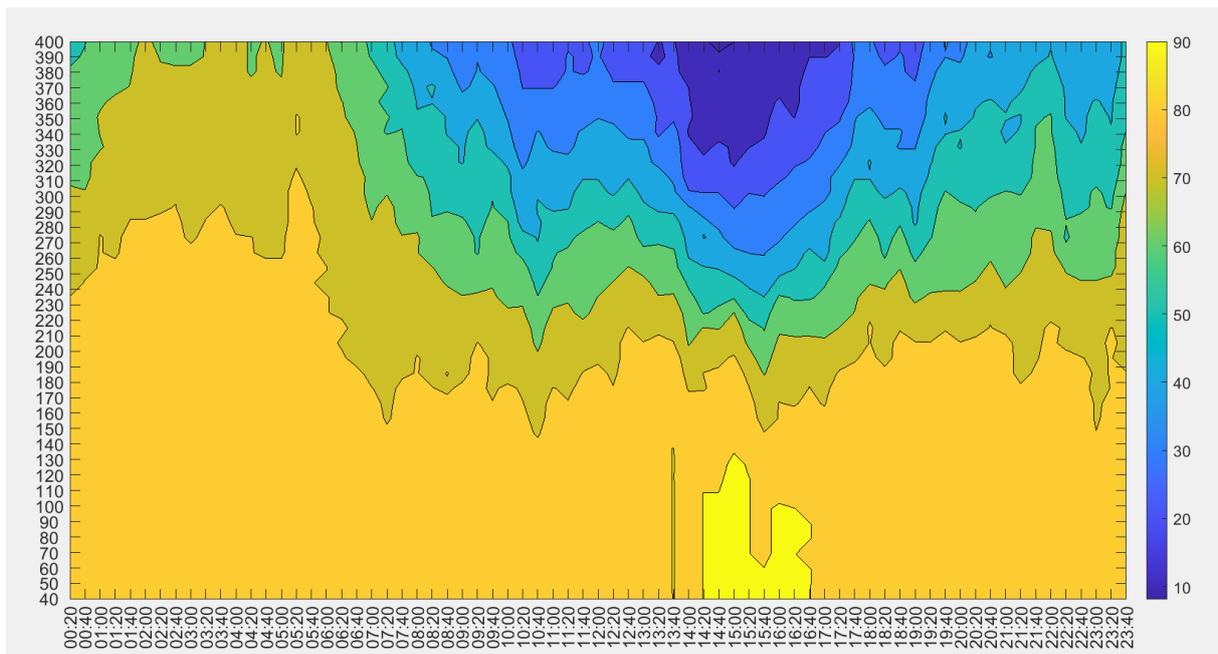
Figure 7 Availability of data (%) in respect to height and time of a day.

Plot shown in Figure 8 provides information of mean wind speed profile in respect to altitude. Mean values were taken for whole period (from 20 June 2022 to 31 November 2022) and averaged over u and v wind component. As expected, magnitude of wind speed increases with height. For the June/July/August there were some small oscilations in LSB circulation, while for the September/October/November oscilation for the LSB circulation are significant. For the case of mean vertical wind profile, the magnitude of wind speed starting from 30 m height is 3.2 m/s, while at height of 400 m, value reaches 5 m/s.
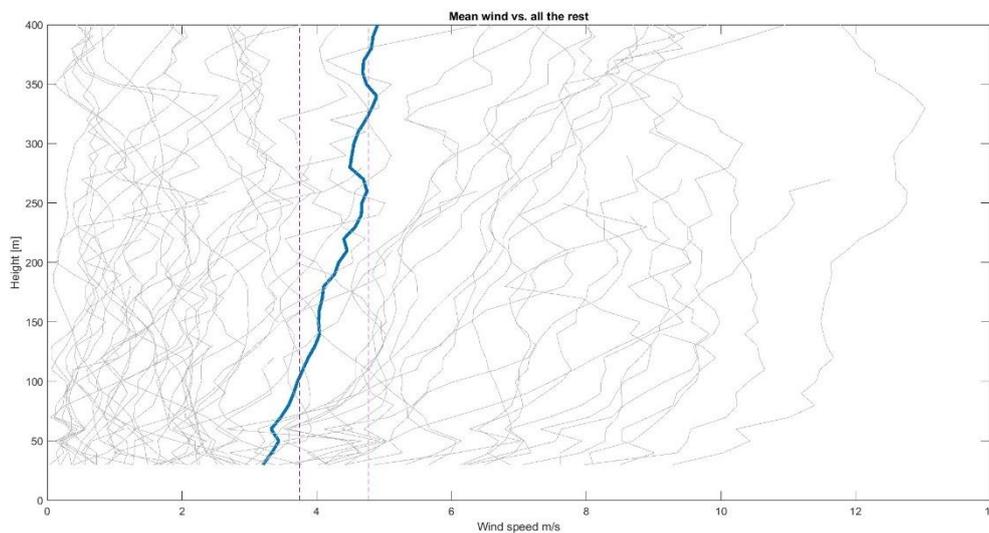
Figure 8 All wind profiles and mean wind profile (dark blue) and standard deviation in vertical dashed purple lines.

Plot shown in Figure 9 and Figure 10 provides information of mean wind speed profile in respect to altitude. Figure 9 represents the period of June-July-August when there were not that many measured wind profiles. One can notice that there were many wind profiles with smaller wind speed (less than 3 m/s) and only a few with wind speed above the value of 4 m/s. The mean wind profile for June-July-August had a value at 30 m altitude $\approx$ 1.8 m/s, while at maximum measured altitude (400 m) value of $\approx$ 3.2 m/s.
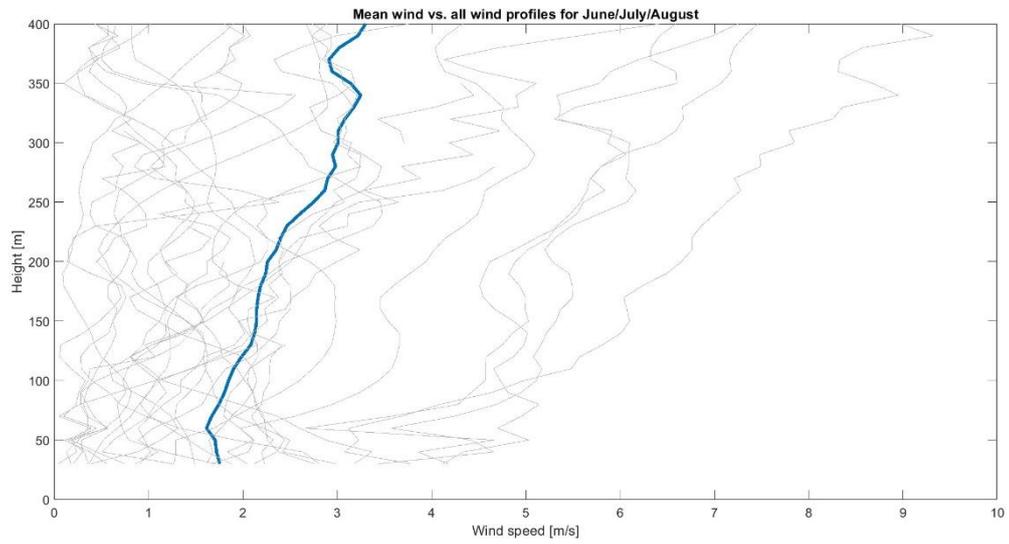
Figure 9 Wind profiles for June-July-August (in grey) and the mean wind profile (in blue).
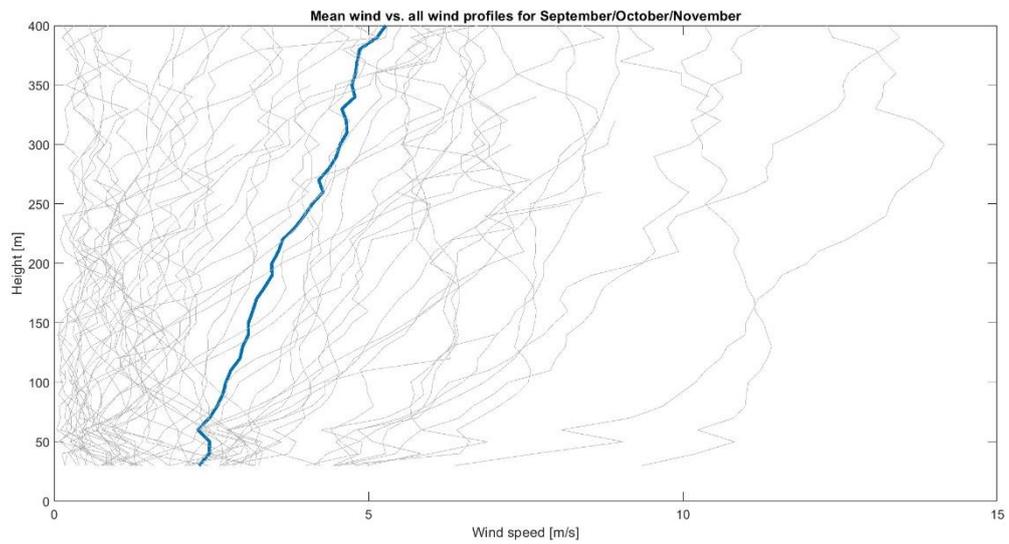
Figure 10 Wind profiles for September-October-November (in grey) and the mean wind profile (in blue).

Figure 10 represents the period of September-October-November when there were more measured wind profiles, as one can notice from the plot. The diversity of wind speeds directly changes the shape of mean wind profile. Mean wind profile on Figure 10 has a starting point at 30 m altitude with wind speed of $\approx$ 2.7 m/s, while at altitude of 400 m has $\approx$ 5.2 m/s. If we take a look at the three figures above (Figure 8, Figure 9 and Figure 10), figure that more suits the mean wind profile for the all wind profiles for whole period (Figure 8) is Figure 10. That one suited the LSBs more and the reason for that might be bigger available data set.

To determine dominant monthly speeds and directions of wind I created monthly wind rose plots for characteristic heights (30 m, 200 m and 400 m). It can be noticed, for each month (June-November), that wind changes its direction from the ground level (30 m height) upwards, regardless of the month.

At ground level (Figure 11a), it can be noticed that the dominant surface (30 m) winds during June were southwesterly exceeding speeds of 10 m/s and southeasterly winds reaching speed of 7 m/s. At height of 200 m (Figure 11b) prevailing winds during June were southeasterly and southwesterly with speeds reaching 8 m/s. In the upper layer (at height of 400 m, in Figure 11c) the situation was quite different: dominant winds were northwesterly reaching speeds up to 12 m/s; southeasterly winds were less frequent reaching speeds up to 12 m/s.

From Figure 11d-f, representing the wind rose for July, it is noticeable that the prevailing winds at the ground level were southeasterly with speeds up to 12 m/s and light southeasterly winds with speeds up to 6 m/s. The situation was different at 200 m (Figure 11e), dominant winds were southeasterly with speeds up to 12 m/s and easterly/northeasterly with speeds up to 8-12 m/s. Going to higher levels, at 400 m (Figure 11f), the prevailing wind was northeasterly wind with speeds up to 14 m/s.

During August, winds at surface level had somewhat different characteristics than during June and August. Nonetheless, there are only 5 days of data for August – thus this plot does not represent a true climatology of August 2022. From Figure 11h two dominant winds at 200 m height were distinguishable: northeasterly with speeds up to 10 m/s and southwesterly wind with speeds up to 8 m/s. At 400 m height (Figure 11i) the winds were mostly northeasterly with speeds up to 12 m/s; northerly winds with speeds up to 14 m/s were also measured.

By comparing June to August wind rose plots, I conclude that at ground level during the three months, dominant winds were southwesterly with speeds up to 10 m/s. At the altitude of 200 m, dominant winds were southwesterly during all three months, and northeasterly during July and August. At height of 400 m, dominant June winds were northerly (northwesterly to northeasterly) and dominant July and August winds were northeasterly.

Table 1 Winds for the June, July and August with given altitude, direction and wind speed.

Month	Height	Prevailing winds	Speeds
June	30 m	southwesterly	10 m/s
		southeasterly	7 m/s
	200 m	southwesterly	8 m/s
		southeasterly	8 m/s
	400 m	northwesterly	12 m/s
		northeasterly	12 m/s
July	30 m	southwesterly	6 m/s
		southeasterly	12 m/s
	200 m	southeasterly	12 m/s
		easterly	8 m/s
		northeasterly	12 m/s
	400 m	northeasterly	14 m/s
August	30 m	southwesterly	7 m/s
		southeasterly	5 m/s
	200 m	northeasterly	8 m/s
		southwesterly	8 m/s
	400 m	northeasterly	12 m/s
		northerly	14 m/s
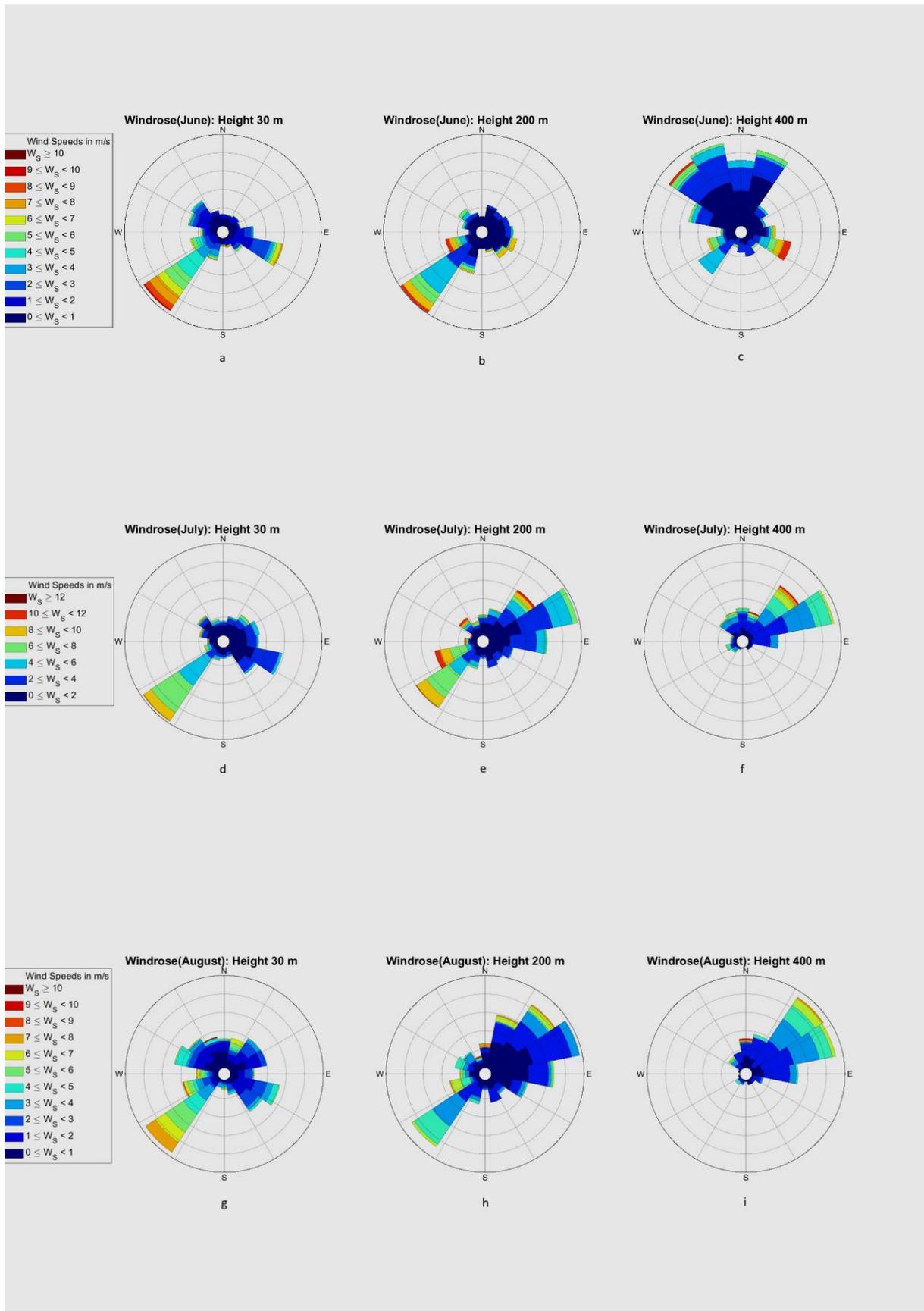
Figure 11 Wind rose plots for June, July, and August for heights of 30, 200 and 400 m.

From Figure 12a one can notice that prevailing ground winds during September were southeasterly ones with speeds up to 10 m/s and northwesterly winds reaching speeds up to 14 m/s. At height of 200 m (Figure 12b) prevailing winds during September were southeasterly with speeds up to 14 m/s. In the upper layer (at height of 400 m in Figure 12c) situation was similar to lower layer: dominant southeasterly wind with speed up to 15 m/s and less dominant northeasterly wind with speeds exceeding 15 m/s.

Figure 12d-f, representing the wind rose for October, it is noticeable that the prevailing winds at height of 30 m were southeasterly with speeds up to 10 m/s and northwesterly with speeds up to 8 m/s. The situation was different at 200 m height (Figure 12e), dominant winds were northeasterly with speeds occasionally greater than 14 m/s and southeasterly ones with speeds up to 12 m/s. From Figure 12f it can be seen that the higher the altitude the greater the wind speeds of prevailing winds: northeasterly and southeasterly winds with speed up to 15 m/s were measured at the highest altitude (400 m).

During November, winds at surface level (Figure 12g) had somewhat different characteristics than in the previous months. There were two dominant winds at surface level northwesterly one with speeds up to 8 m/s and southeasterly one with speeds up to 14 m/s. At height of 200 m (Figure 12h) prevailing wind was southeasterly with speeds reaching more than 15 m/s. Figure 12i reveals dominant winds at height of 400 m, southeasterly wind exceeding speeds of 15 m/s and northwesterly wind with speeds reaching more than 10 m/s.

From Figure 12 we can notice that in all three months (September-October-November) the most frequent surface wind was southeasterly wind with speeds reaching up to 8-16 m/s. During October and November, northwesterly wind was also quite common. This is different from June to August when prevailing wind was southwesterly. At altitude of 200 m the prevailing winds were also southeasterly, again quite different than what was measured in June to August. At height of 400 m, dominant winds during September and October were southeasterly and northeasterly with speeds up to 7-9 m/s.

In November, however, northwesterly winds were most frequent. Characteristic wind speeds reached up to 10-12 m/s. By examining the monthly wind roses, we can follow and study changes between the months and between summer and autumn season. However, to make stronger conclusions on typical behaviour we need to have longer sets of measurements.

Table 2 Winds for the September, October and November with given altitude, direction and wind speed.

Month	Height	Prevailing winds	Speeds
September	30 m	southeasterly	10 m/s
		northwesterly	14 m/s
	200 m	southeasterly	14 m/s
	400 m	southeasterly	15 m/s
		northwesterly	15 m/s
October	30 m	southeasterly	10 m/s
		northwesterly	8 m/s
	200 m	northeasterly	14 m/s
		southeasterly	12 m/s
	400 m	northeasterly	15 m/s
		southeasterly	
November	30 m	northwesterly	8 m/s
		southeasterly	14 m/s
	200 m	southeasterly	15 m/s
	400 m	southeasterly	15 m/s
		northwesterly	10 m/s
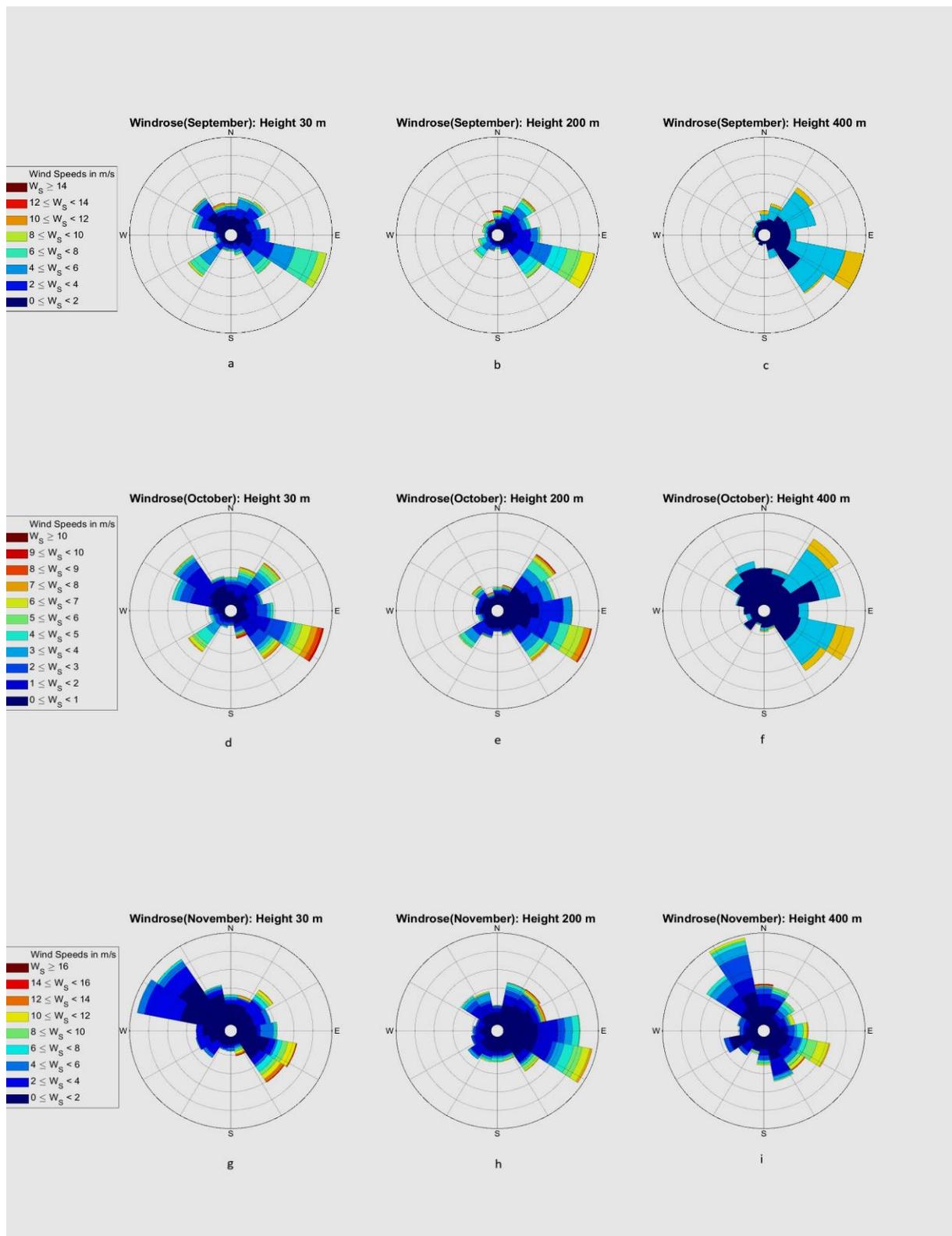
Figure 12 Wind rose plot for September, October, and November for heights of 30, 200 and 400 m.

4.2 Characteristic winds

I have derived criteria for extracting characteristic winds based on literature and specific characteristics of local winds at the Split airport [2], [7], [8], [9]. I used two criteria, one based on speed and direction (Table 3) and the other based only on direction of wind (Table 3). [11],[12] Both criteria were applied to 30 m data. Percentages of situations with sirocco wind, bora wind, sea breeze, and land breeze are given in Figure 13. For my analysis I decided to use both "no speed criteria"and "speed criteria".

Table 3 Criteria to determine dominant winds.

WIND	SEA BREEZE	LAND BREEZE	SIRROCCO	BORA
SPEED CRITERIA (m/s)	> 6	> 6	> 10	> 10
DIRECTION CRITERIA $(^0)$	$[180 - 235]$	$[0 - 90]$	$[105 - 165]$	$[25 - 75]$
WIND	SEA BREEZE	LAND BREEZE	SIRROCCO	BORA
NO SPEED CRITERIA (m/s)	$\sim$	$\sim$	$\sim$	$\sim$
DIRECTION CRITERIA $(^0)$	$[180 - 235]$	$[0 - 90]$	$[105 - 165]$	$[25 - 75]$
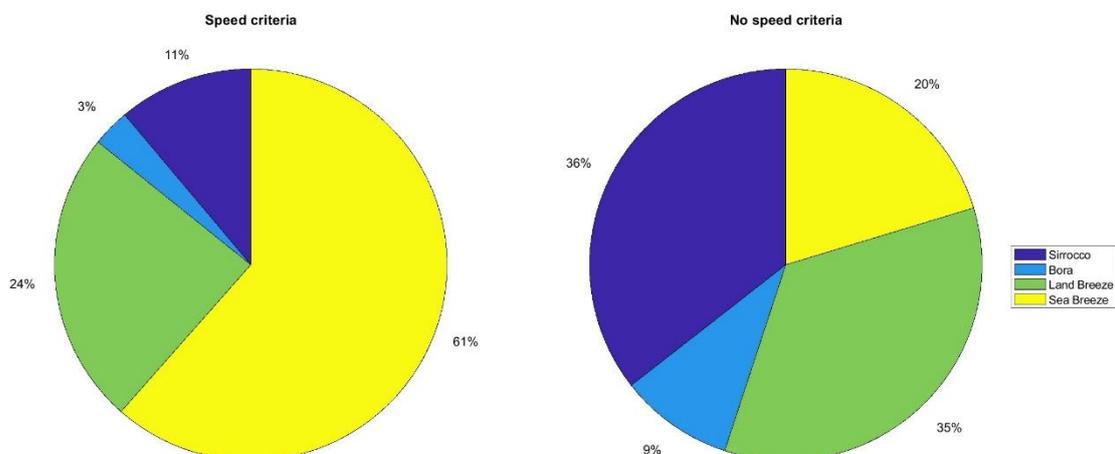
Figure 13 Pie charts for dominant winds according to (left) „speed criteria", (right) „no speed criteria".

Typical values of sea breeze are 6 m/s and using the Table 3 for wind speed criteria, Figure 13 (left) is prevailing with sea breeze ≈61%. When the wind speed criteria is removed (Figure 13 right), dominant wind became land breeze ≈35%. The main reason for that is since the provided data are stacked with small velocity values and common values for land breeze are 2.5 to 4 m/s (5.8 knots).

Since the data analysed was mostly measured during summer season, as one can expect less frequent episodes of bora/sirocco winds and more frequent land and sea breeze winds. Using the wind speed criteria (Figure 13 left) for the data provided prevailing winds were sea breeze (61%) and land breeze (24%). When wind speed criteria is removed, all winds become more evenly distributed (Figure 13 right) including sirocco and bora winds. Temporal distribution of local winds over the investigated period is also shown in Figure 14 confirming again prevalence of the land and sea breeze ("speed criteria" from Table 3 were used to extract the winds). There were 12 episodes of bora wind, 43 episodes of jugo/sirocco, 94 episodes of sea breeze and 238 episodes of land breeze with respect to heights.
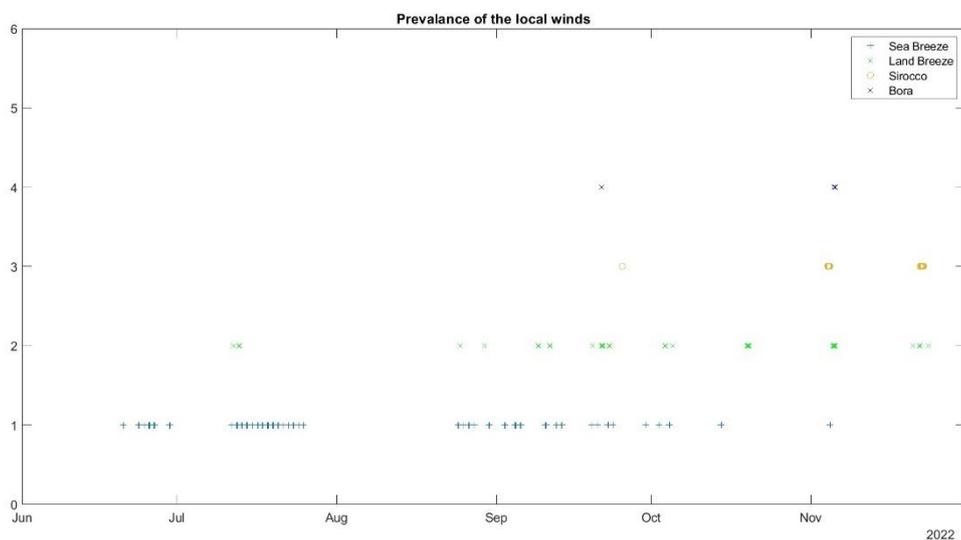
Figure 14 Prevalence of the local winds.

4.3 Sea breeze – Land breeze circulation (LSBs)

During the summer season, as seen from wind rose plots (Figure 11 and Figure 12), and from Figure 13 and Figure 14, dominant wind patterns at the Split airport are land and sea breeze. To evaluate their circulation (LSBs) in more detail, a code in MATLAB for visualization of winds was developed. In Figures 15 and 16 I show mean wind speed and direction profiles during 26 days with sea breeze. In Figure 17, I show wind profiles as given by the MFAS SODAR software (APRun) for 11-12 July 2022. From all plots, it can be seen that sea breeze starts around 15:00 CET and it lasts till ~23:00 CET, and land breeze starts to cancel the sea breeze during the night hours (22:00-06:00 CET). Changes in wind direction as previously seen on wind rose plots, now can be seen for the mean land and sea breeze events in Figure 17.
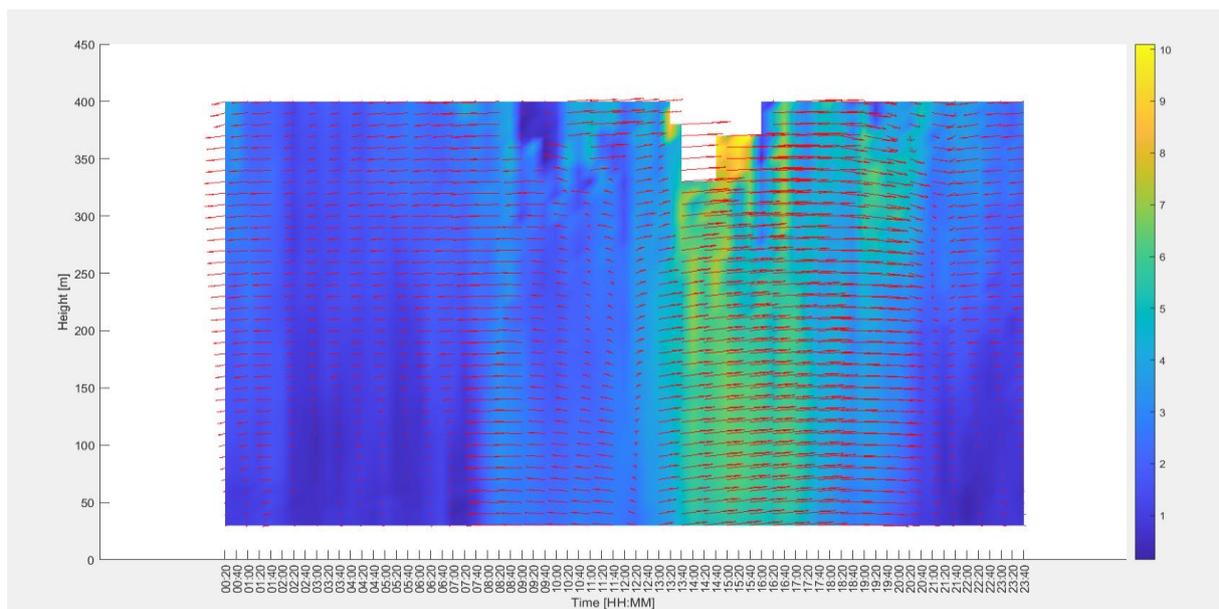
Figure 15 Mean wind profile estimated for days during which sea breeze occurred. Colours denote speed (m/s) and arrows denote direction. Direction is better seen in Figure 14.
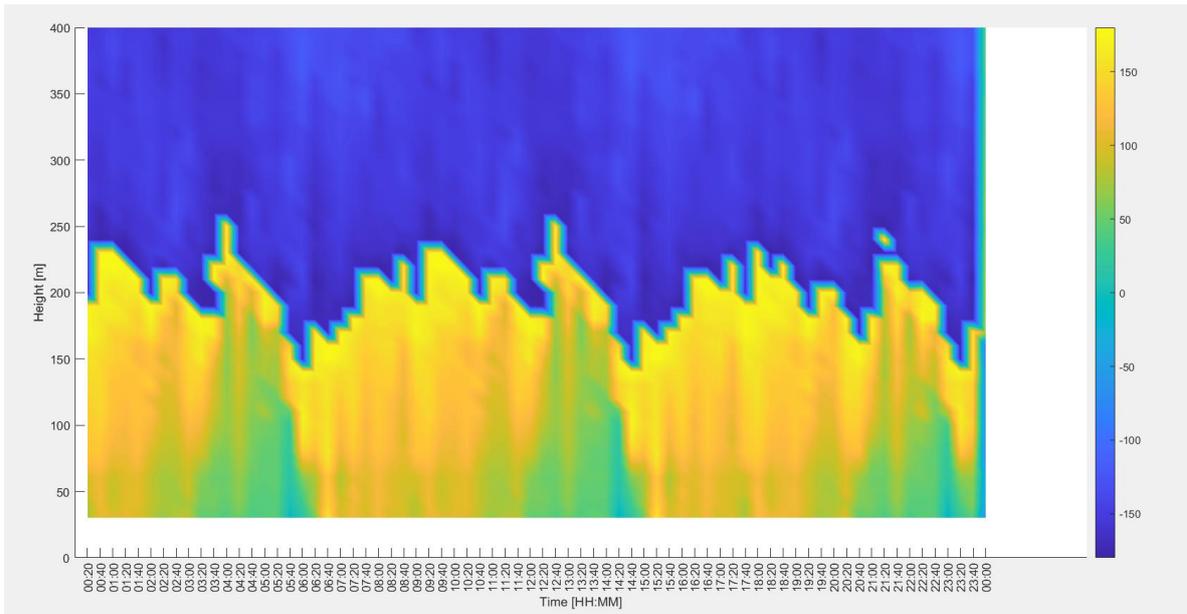
Figure 16 Mean profile of wind direction estimated for days during which sea breeze occurred. Colours denote direction (°) with 0° marking easterly winds; 90° marking southerly winds; 180° marking westerly winds; -90° marking northerly winds.
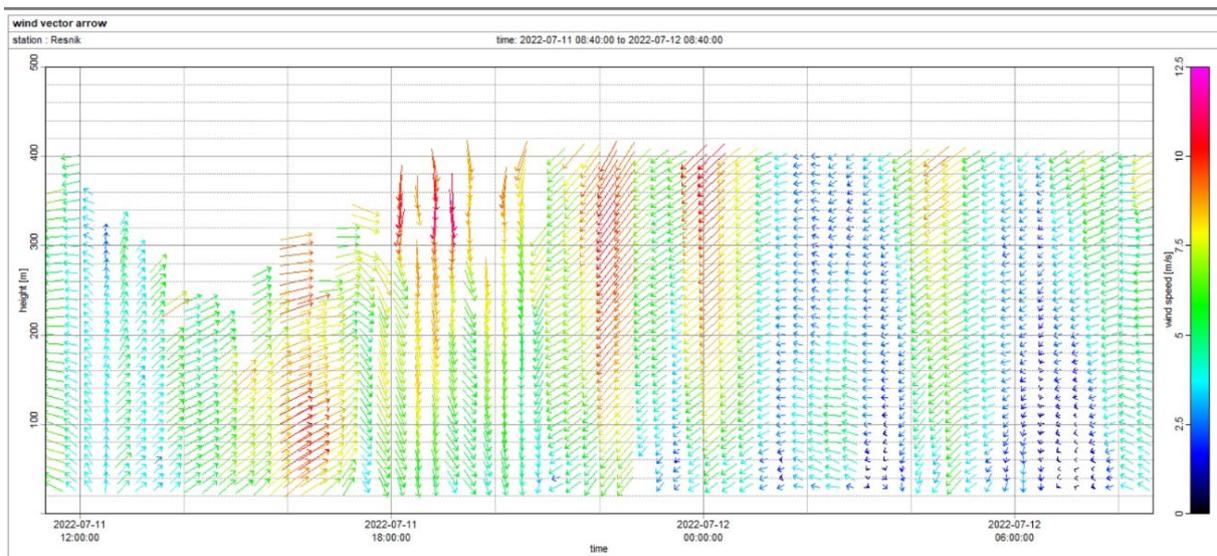
Figure 17 Wind profiles for 11-12 July 2022. Plot was downloaded directly from MFAS SODAR APRun software.

Figure 17 was taken when the typical situation of land and sea breeze circulation occurred. At 15:00 CET one can observe the start of a sea breeze, which tends to cancel out at 22:00 CET (when land breeze started to occur) and this circulation is something specific that occurs during the summer along the coast. This can again be explained by the differential heating of air over Split and Adriatic Sea. As the sun heats the boundary layer over land (Split), the resulting pressure gradient causes the movement of low- level air from the Adriatic to the land.

5 ERA5 data reanalysis

5.1 Typical synoptic setting of land and sea breeze (June-November)

To better understand the synoptic setting related to land and sea breezes occurrence, I examined both: in situ measurement and the ERA5 reanalysis data. By evaluating the mean sea level pressure (MSLP) and 500 hPa geopotential height as obtained from ERA5, I found out what kind of synoptic situations are suitable for occurrence of land and sea breeze in the Adriatic Sea. I show the ERA5 charts at two moments of the day: 15:00 CET, when sea breeze starts to develop and at 23:00 CET, when land breeze starts. To describe characteristic synoptic conditions, mean values of the events when LSBs occurred and averaged for all days per month were considered.

For a sea breeze circulation to occur, the synoptic scale pressure spatial gradient must be quite weak, because if there are strong synoptic scale pressure gradients related winds will overwhelm sea breeze circulation. The relative importance of land – sea circulation is shown using pressure gradient, magnitude of wind and wind direction on the plots bellow. Over the area of Croatia, the average MSLP fields on days when there was sea breeze are rather uniform, showing no pronounced spatial gradients. Table 4 shows number of days with and without land and sea breeze circulation during the investigated period. The reason why the sum of days with and without LSB does not sum up to number of days in a month is because of the missing data.

Table 4 Number of days of whole data set when LSB either occurred or not for in situ measurements.

Months	Number of days	
	with LSB	without LSB
June	2	9
July	11	4
August	3	6
September	4	26
October	5	20
November	1	21

In Figure 18 I show mean MSLP and 10-m wind, and in Figure 19, 500 hPa geopotential height and wind, in upper rows for June days during which sea breeze occurred, and in lower rows for the entire June 2022. The same is shown in Figures 20 to 28 for July to November. For November, there was only one sea breeze day (Table 4, Figure 28).

In June, LSB days are characterized by weak spatial pressure gradient (isobars determining the pressure system were not close, but far apart) over the Mediterranean, whereas for the entire June there was a land-sea pressure gradient with higher pressure over the land (noticeable at both 15:00 and 23:00 CET).
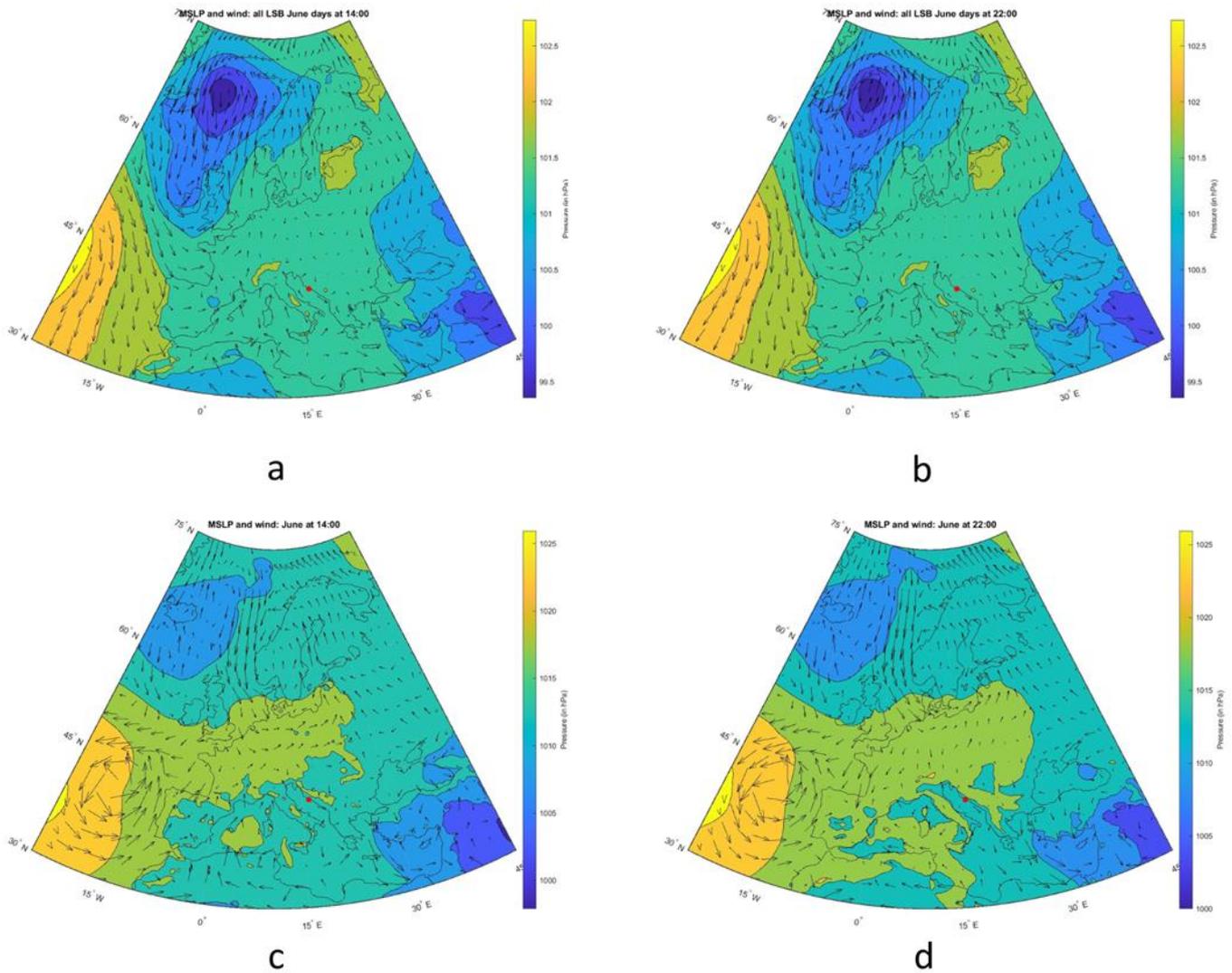
Figure 18 Averages of mean sea level pressure and wind estimated for: a) 14:00 UTC of June 2022 days with LSB, b) 22:00 UTC of June 2022 days with LSB, c) 14:00 UTC of all June 2022 days and d) 22:00 UTC of all June 2022 days.

As for 500 hPa geopotential height, I see no significant difference between sea breeze days, and the rest of days in a month, over the Adriatic Sea (Figure 19). Over the area of Split, Figure 19a and Figure 19b is located in the same contour of geopotential height of 5800 m. All June days, for geopotential height of 500 hPa above Split, shows slightly bigger value of geopotential height of 5850 m. Contours over the Croatia are not that close by, so there is not to expect a strong wind over the Adriatic. Nonetheless, over the northern Europe, noticeably lower geopotential heights were present on days without sea breeze.
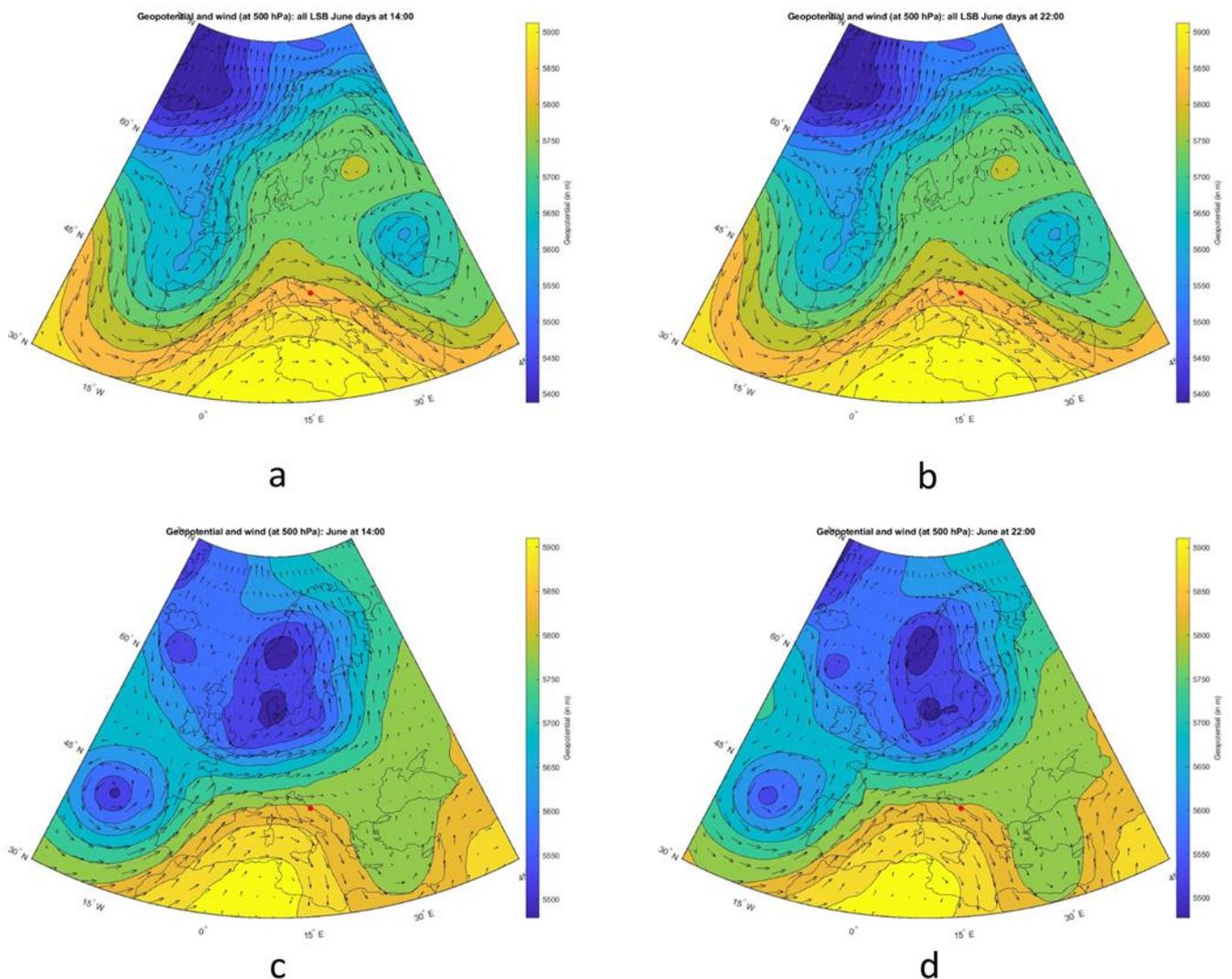
Figure 19 Averages of mean 500 hPa level wind estimated for: a) 14:00 UTC of June 2022 days with LSB, b) 22:00 UTC of June 2022 days with LSB, c) 14:00 UTC of all June 2022 days and d) 22:00 UTC of all June 2022 days.

The average MSLP and 10-m wind plots for LSB days in July 2022 reveal again that there were no significant pressure gradients over the Adriatic Sea (for LSB days in July values over Split were 1010 hPa Figure 20a and Figure 20b). Since there were no close by contours above Croatia, one cannot expect strong winds. Averages estimated for the entire month had similar values of pressure gradient 1015 hPa (with higher pressure over the mountainous area of Croatia shown in Figure 20c and Figure 20d).
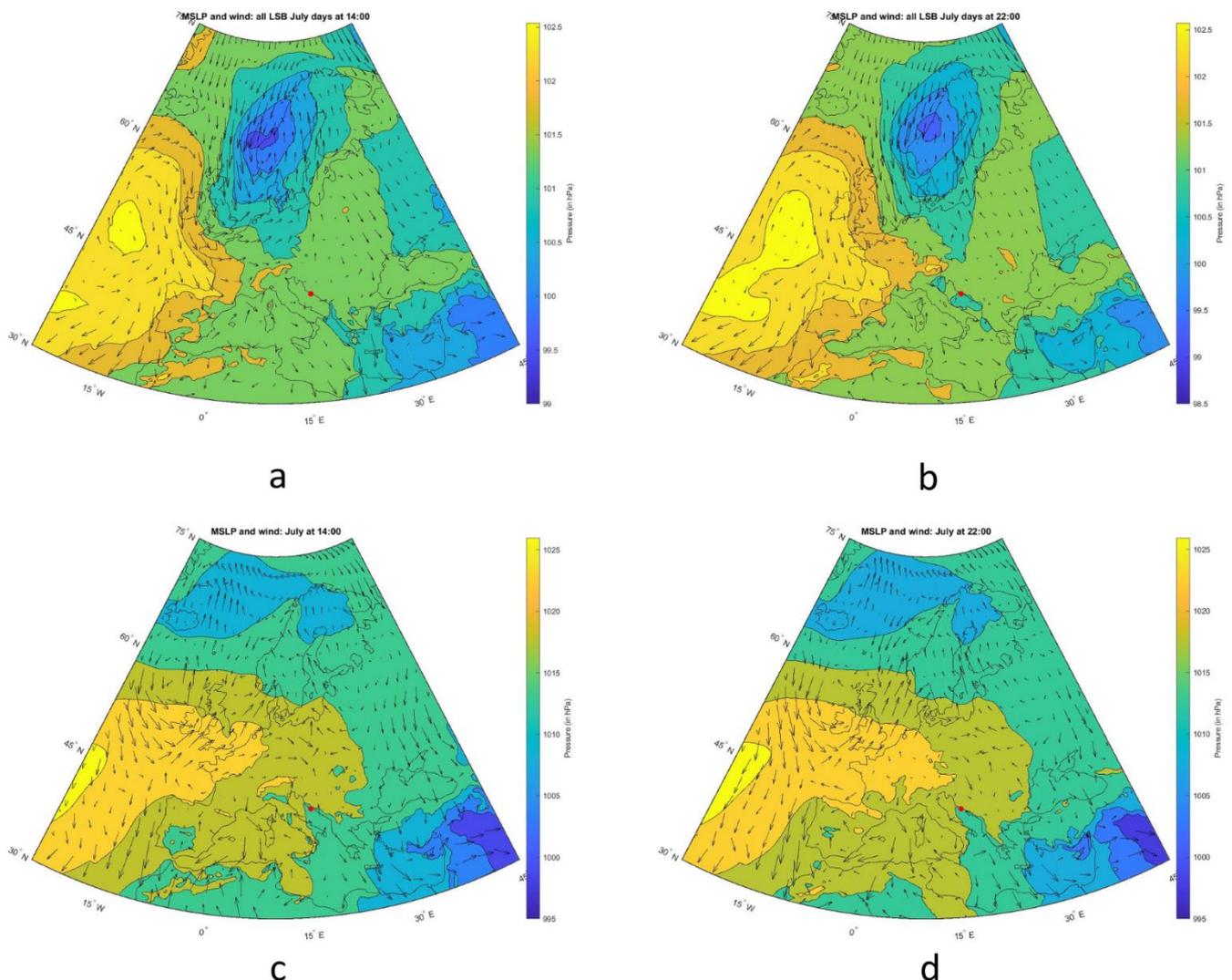
Figure 20 Averages of mean sea level pressure and wind estimated for: a) 14:00 UTC of July 2022 days with LSB, b) 22:00 UTC of July 2022 days with LSB, c) 14:00 UTC of all July 2022 days and d) 22:00 UTC of all July 2022 days.
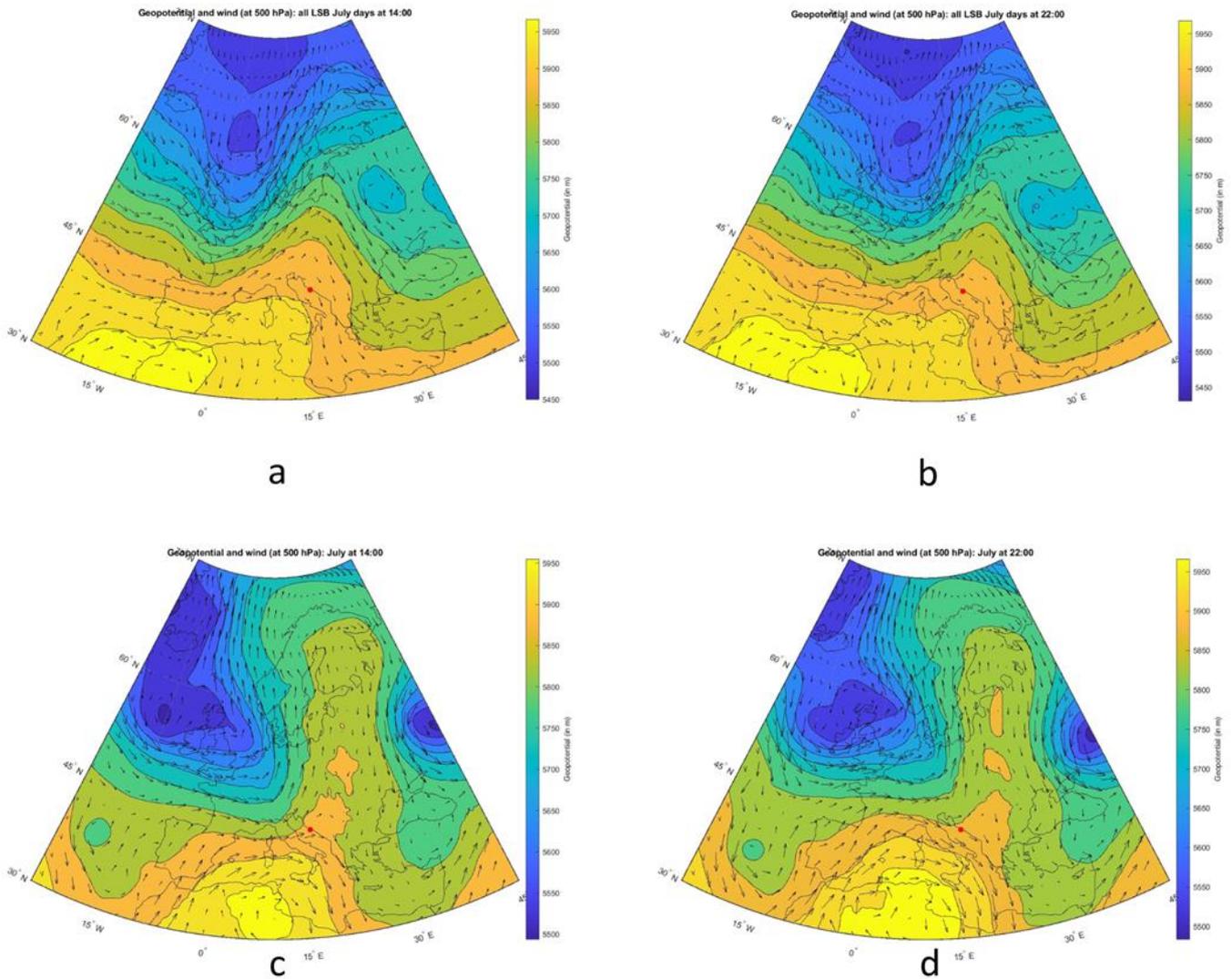
Figure 21 Vector plot with surface plot providing pressure in hPa for July at 500hPa. Four cases are shown: a) averaged LSB days at 14:00, b) averaged LSB days at 22:00, c) monthly average of all days at 14:00 and d) monthly average of all days at 22:00.

As for 500 hPa geopotential height, the situation during LSB days in July 2022 was similar to the situation during LSB days in June 2022 (Figure 21). For the entire month of July 2022, one can notice a distinct trough and ridge structure to the north of the Mediterranean.
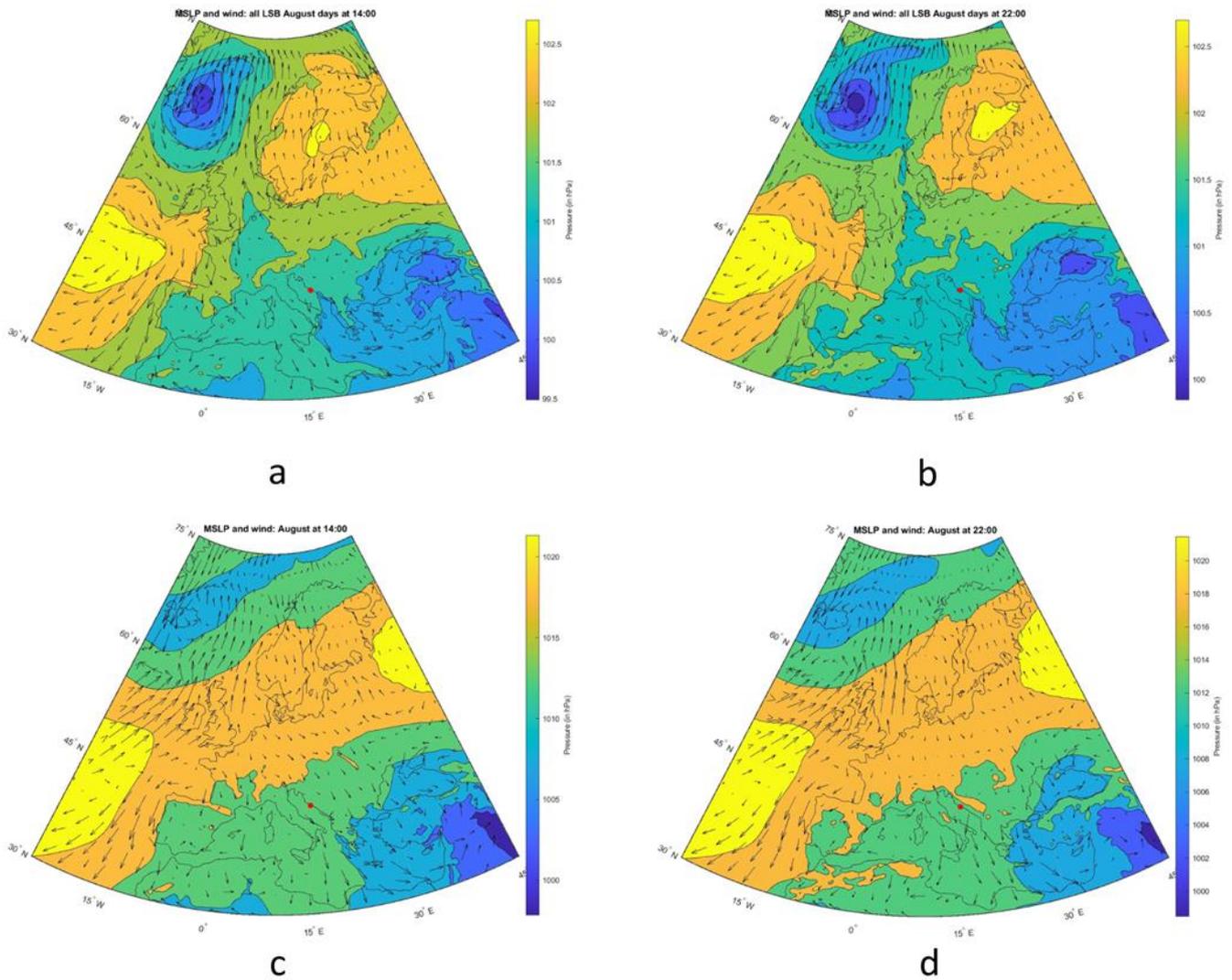
Figure 22 Averages of mean sea level pressure and wind estimated for: a) 14:00 UTC of August 2022 days with LSB, b) 22:00 UTC of August 2022 days with LSB, c) 14:00 UTC of all August 2022 days and d) 22:00 UTC of all August 2022 days.

In Figure 22 I show mean MSLP and 10-m wind, and in Figure 23, 500 hPa geopotential height and wind, in upper rows for August days during which sea breeze occurred, and in lower rows for the entire August 2022.

In August, LSB days were characterized by weak spatial gradients over the Mediterranean, whereas for the entire August there was a land-sea pressure gradient with higher pressure over the land (noticeable at both 15:00 CET and 23:00 CET. As for the MSLP over Split, values were 1015 hPa with distant contours.

As for the 500 hPa geopotential height, I see no significant difference between sea breeze days, and the entire month, over the Adriatic Sea (Figure 23). Figure 23a and Figure 23b, unlike the Figure 23c and Figure 23d were provided with small low pressure area above Greece. Geopotential height remained 5800 m with come close by conoturs above Greece. Having that in mind, one can expect wind coming from area of high pressure area to low pressure area (from Croatia to Greece). Nonetheless, over the continental Europe, noticeably higher geopotential heights (5850 m) were present on days with sea breeze.
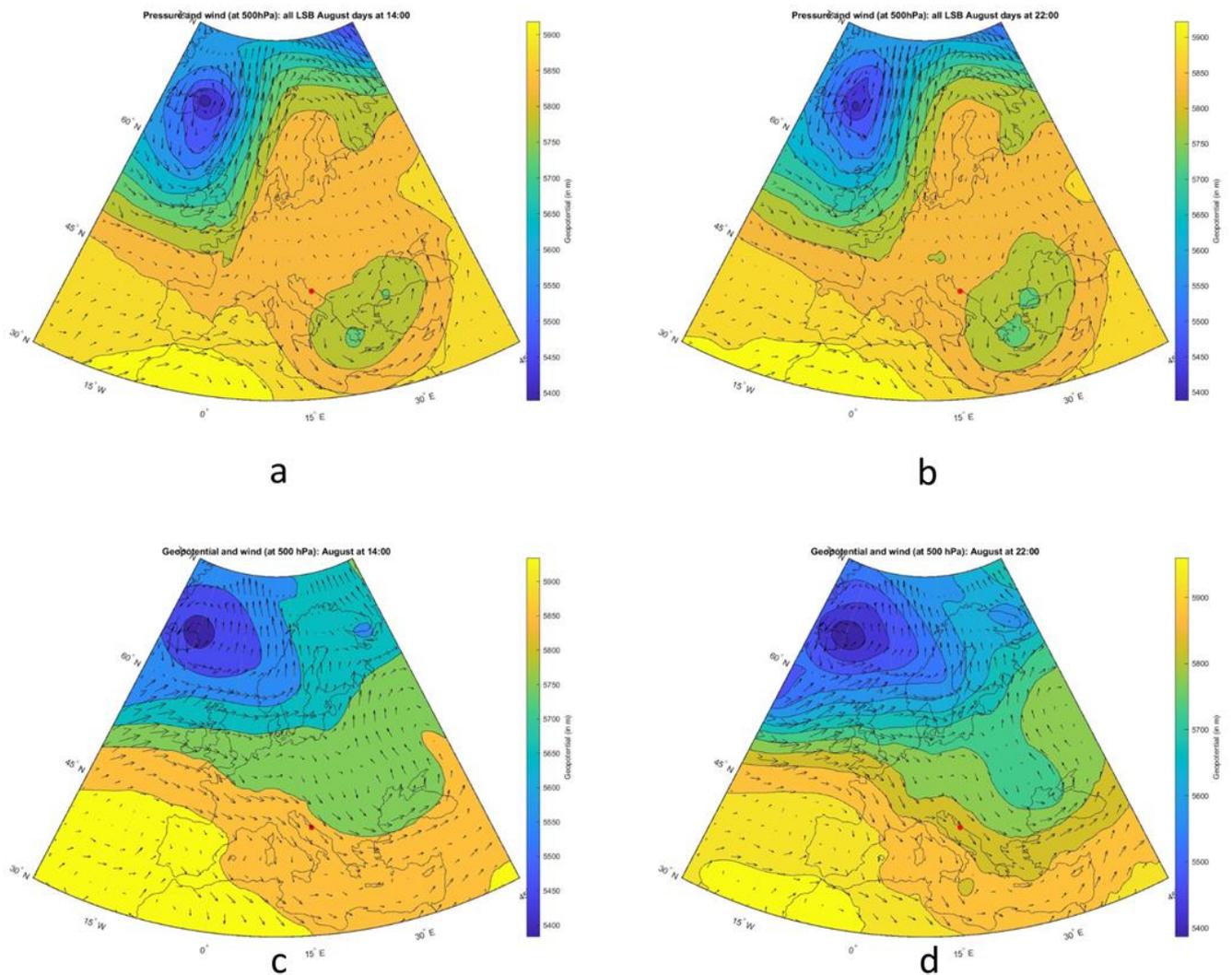
Figure 23 Averages of 500 hPa level pressure and wind estimated for: a) 14:00 UTC of August 2022 days with LSB, b) 22:00 UTC of August 2022 days with LSB, c) 14:00 UTC of all August 2022 days and d) 22:00 UTC of all August 2022 days.

The average MSLP and 10-m wind plots for LSB days in September 2022 reveal again that there were no significant pressure gradients over the Adriatic Sea, the situation during LSB days in September 2022 was like situation during LSB days in August 2022. For 500 hPa geopotential height, I see no significant difference between sea breeze days (values of MSLP were 1015 hPa with high level pressure over the Sweden and Atlantic Ocean; 1020 hPa, low pressure area over Turkey; 1005hPa), and the entire month, over the Adriatic Sea (Figure).
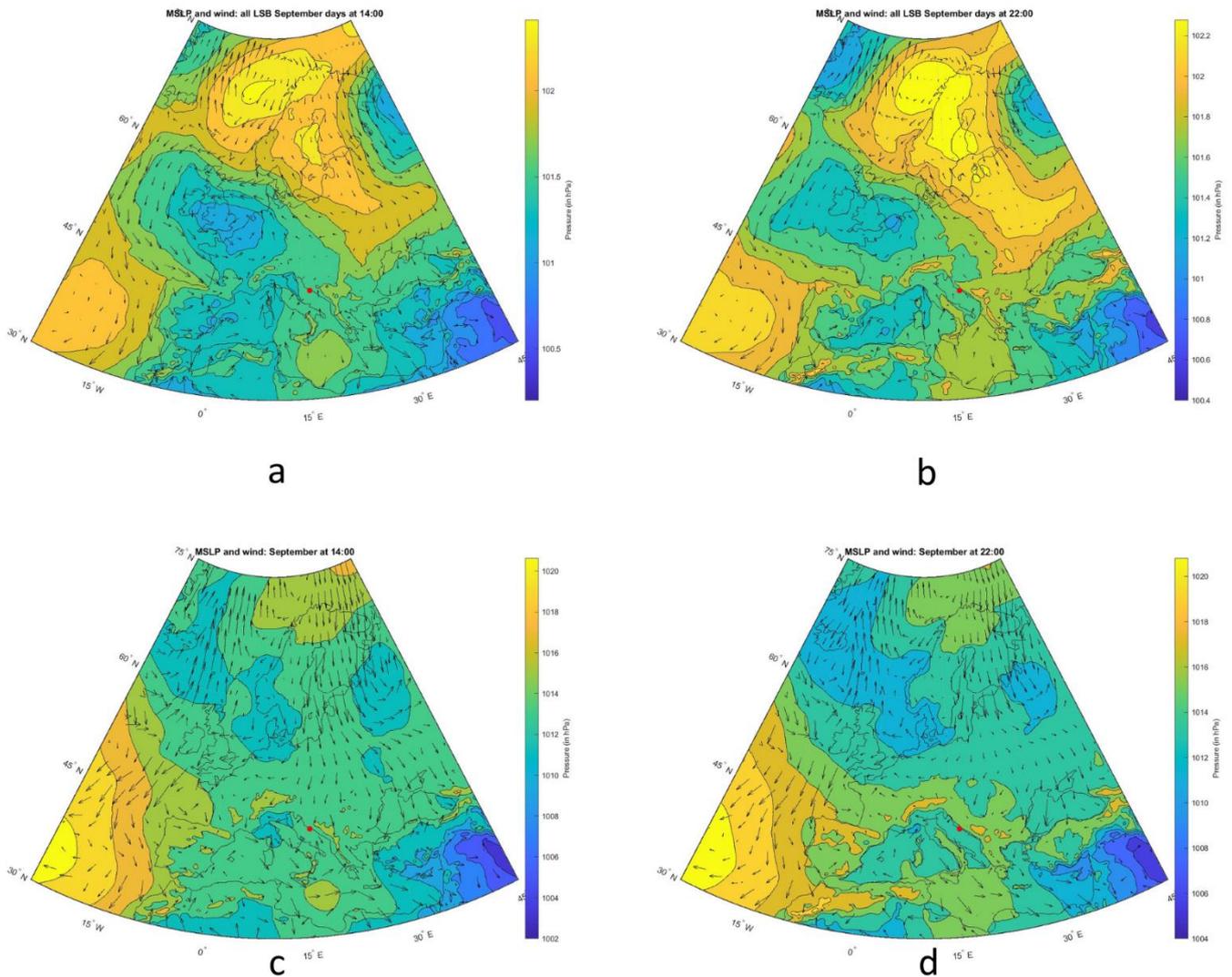
Figure 24 Averages of mean sea level pressure and wind estimated for: a) 14:00 UTC of September 2022 days with LSB, b) 22:00 UTC of September 2022 days with LSB, c) 14:00 UTC of all September 2022 days and d) 22:00 UTC of all September 2022 days.

As for 500 hPa geopotential height (Figure 25), the situation during LSB days in September 2022 was like situation during LSB days in August 2022. For 500 hPa geopotential height, there were some close by streamlines 5700/5750/5800 m above Croatia, meaning that some wind can be expected from the south to the north of the country.
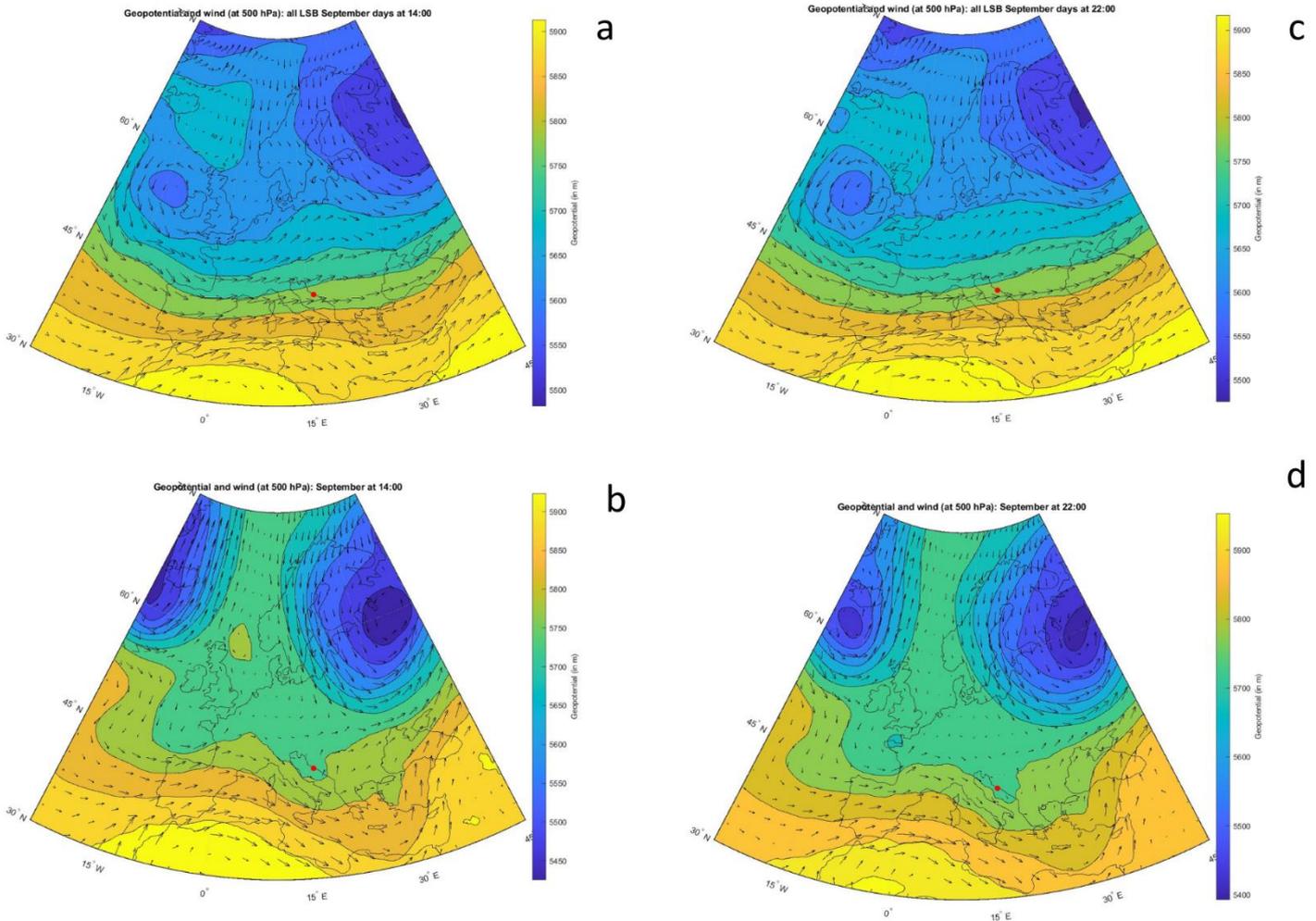
Figure 25 Averages of mean 500 hPa level pressure and wind estimated for: a) 14:00 UTC of September 2022 days with LSB, b) 22:00 UTC of September 2022 days with LSB, c) 14:00 UTC of all September 2022 days and d) 22:00 UTC of all September 2022 days.

In Figure 26, I present the Mean Sea Level Pressure (MSLP) and 10-meter wind data for October, and in Figure 27 the 500 hPa geopotential height and wind patterns. The upper rows represent October days with sea breeze events, while the lower rows depict the entire month of October 2022.

During October sea breeze days, there were weak spatial MSLP gradients over the Mediterranean. There were 1020 hPa MSLP northwesterly of Split and just by moving a bit to the south there were 1015 hPa MSLP indicating wind moving from the north to the south. However, throughout October, there is a notable north-to-south pressure gradient, leading to higher pressure over the Mediterranean and lower pressure over the Atlantic and northern Europe, which is evident at both 15:00 CET and 23:00 CET.

Streamlines shown on Figure 27a closer by contours than the ones on Figure 27b, indicating stronger winds coming from the southwest. On figures below (for whole October Figure 27c and Figure 27d) there can be noticed small low pressure (5600 m) rigde just above the Split indicating wind coming from the south (higher values; 5900 m)to cancel out the low pressure area.
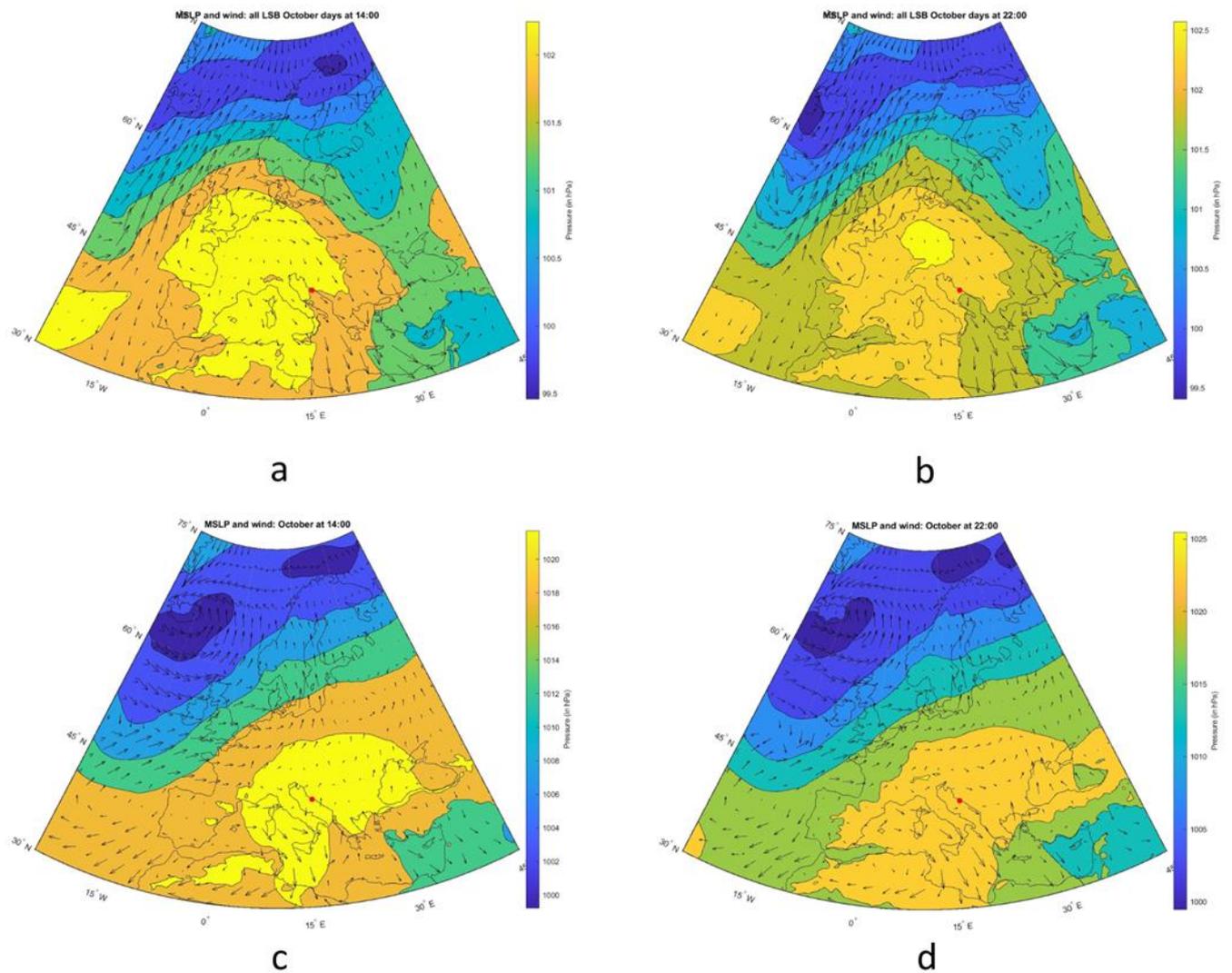
Figure 26 Averages of mean sea level pressure and wind estimated for: a) 14:00 UTC of October 2022 days with LSB, b) 22:00 UTC of October 2022 days with LSB, c) 14:00 UTC of all October 2022 days and d) 22:00 UTC of all October 2022 days.
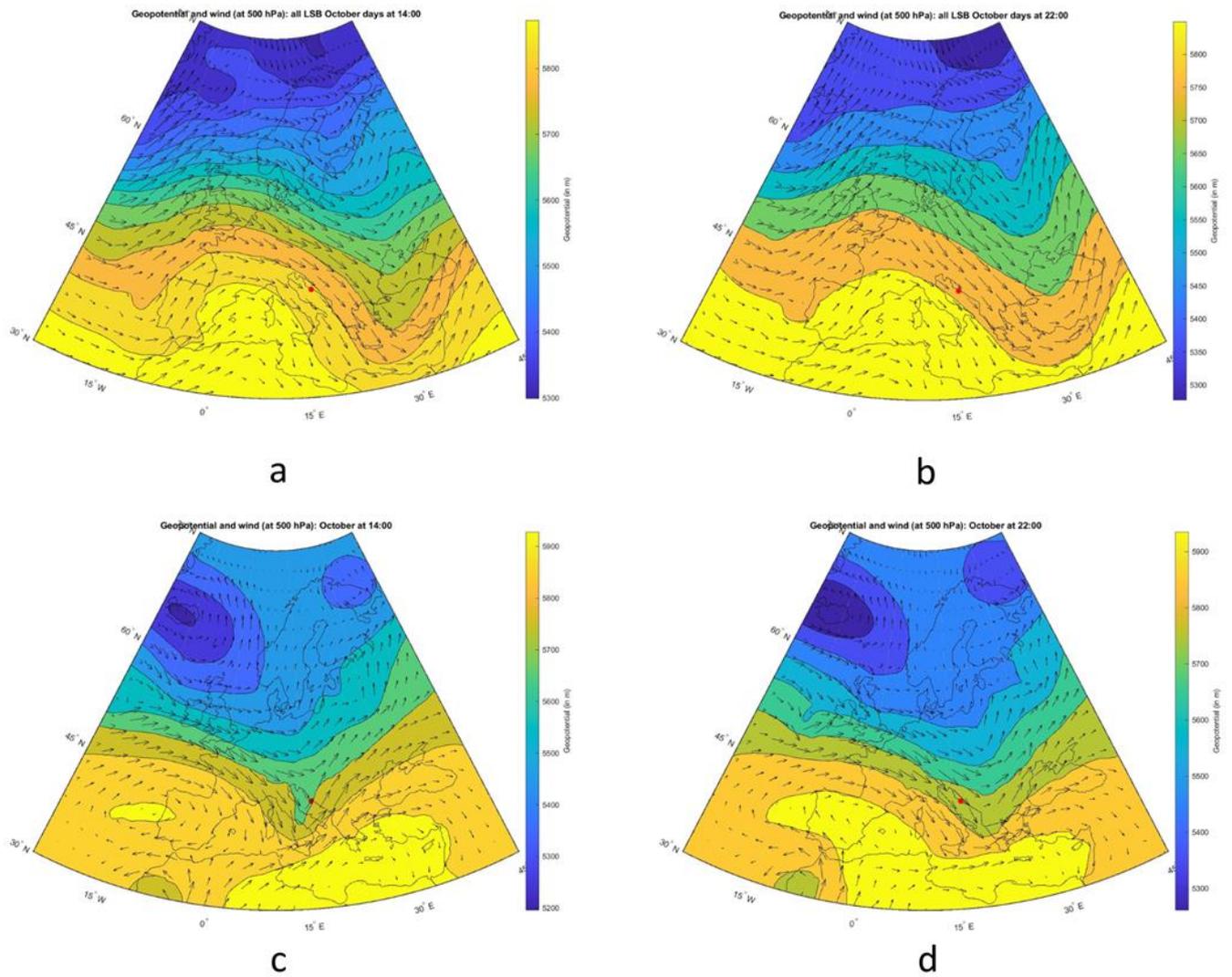
Figure 27 Averages of 500 hPa level pressure and wind estimated for: a) 14:00 UTC of October 2022 days with LSB, b) 22:00 UTC of October 2022 days with LSB, c) 14:00 UTC of all October 2022 days and d) 22:00 UTC of all October 2022 days.

Figure 28 illustrates the 500 hPa geopotential height for November, indicating no significant differences between sea breeze days and the entire month.
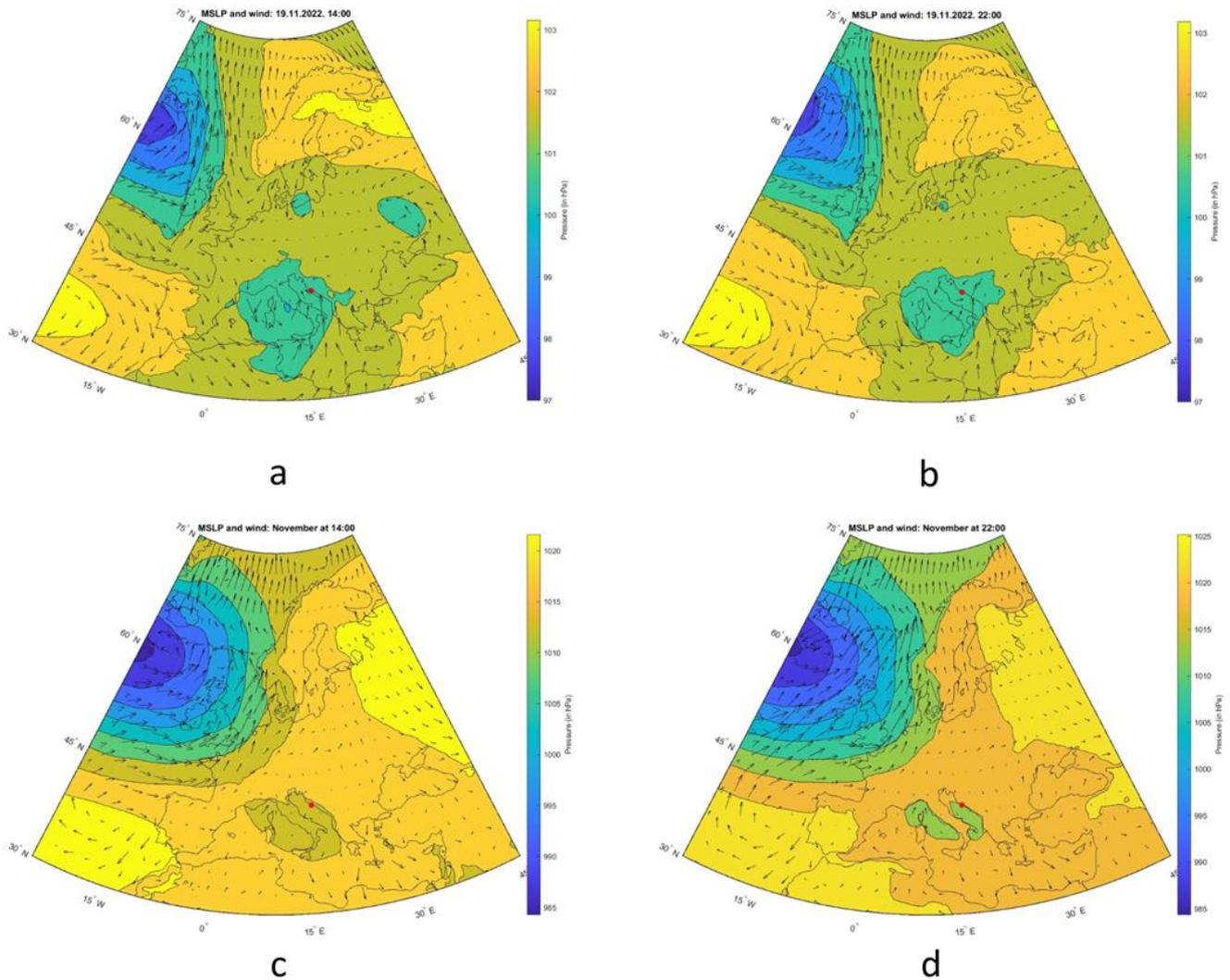
Figure 28 Averages of mean sea level pressure and wind estimated for: a) 14:00 UTC of November 2022 days with LSB, b) 22:00 UTC of November 2022 days with LSB, c) 14:00 UTC of all November 2022 days and d) 22:00 UTC of all November 2022 days.

If we take a closer look to the MSLP on 19 November 2022, the only day in November 2022 when sea breeze occurred, immediately we can notice an area of relatively low pressure above Italy and Croatia (1010 hPa), but weak pressure gradients over the Adriatic Sea (Figure 28).

As for 500 hPa geopotential height, I see low pressure ridge penetrating to the south of France (Figure 29a and Figure 29b), while lower figures (for the entire month) shows completely uniform higher geopotential above the Adriatic; 5750m (Figure 29).

a

b

c

d
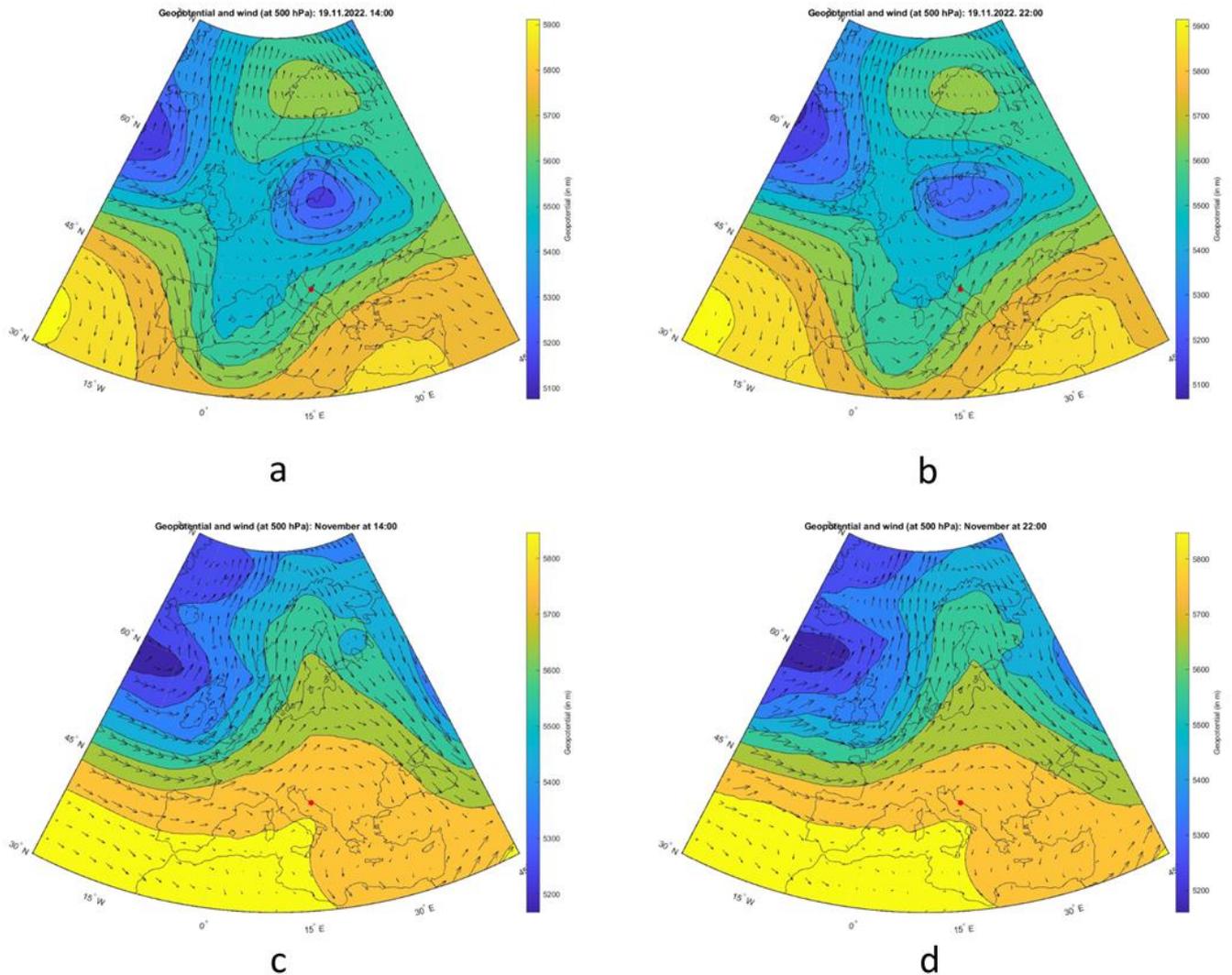
Figure 29 Averages of 500 hPa level pressure and wind estimated for: a) 14:00 UTC of November 2022 days with LSB, b) 22:00 UTC of November 2022 days with LSB, c) 14:00 UTC of all November 2022 days and d) 22:00 UTC of all November 2022 days.

The text describes meteorological conditions during specific months (June to November) in the Mediterranean, particularly focusing on the Adriatic Sea, and the presence or absence of sea breeze. Here is a summary of the key points:

June:

- Weak spatial pressure gradient over the Mediterranean during sea breeze days.

- Land-sea pressure gradient with higher pressure over the land for the entire month.

- No significant difference in 500 hPa geopotential height between sea breeze and non-sea breeze days.

July:

- Weak spatial pressure gradients over the Adriatic Sea during sea breeze days.

- Land-sea pressure gradient for the entire month with higher pressure over the land.

- No significant difference in 500 hPa geopotential height between sea breeze and non-sea breeze days.

August:

- Similar conditions to July with weak spatial pressure gradients during sea breeze days.

- Land-sea pressure gradient for the entire month with higher pressure over the land.

- No significant difference in 500 hPa geopotential height between sea breeze and non-sea breeze days.

September:

- Similar conditions to August with weak spatial pressure gradients during sea breeze days.

- Land-sea pressure gradient for the entire month with higher pressure over the land.

- Some wind expected from the south to the north of Croatia based on 500 hPa geopotential height.

October:

- Weak spatial MSLP gradients over the Mediterranean during sea breeze days.

- North-to-south pressure gradient for the entire month.

- Streamlines suggest stronger winds from the southwest during sea breeze days.

November:

- No significant differences in 500 hPa geopotential height between sea breeze days and the entire month.
- On the day sea breeze occurred, a low-pressure area above Italy and Croatia with weak pressure gradients over the Adriatic Sea.

The analysis primarily focuses on pressure gradients, geopotential height, and wind patterns during sea breeze days compared to the entire month, providing insights into the atmospheric conditions influencing sea breeze events in the Mediterranean region.

5.2 Episode with LSB 11 July 2022.

To take a deeper look into the LSB circulation, a specific date during the summer season was chosen. The measurements from MFAS SODAR for 11 July 2022 are plotted in Figure 30 below. Using ERA5 data we again examine two moments: 15:00 CET and 23:00 CET, where at 15:00 CET we can notice sea breeze, blowing from the sea to the land (Figure 31a). At 23:00 CET wind direction changed and the wind was now blowing from the land to the sea as can be seen in the Figure 31b.
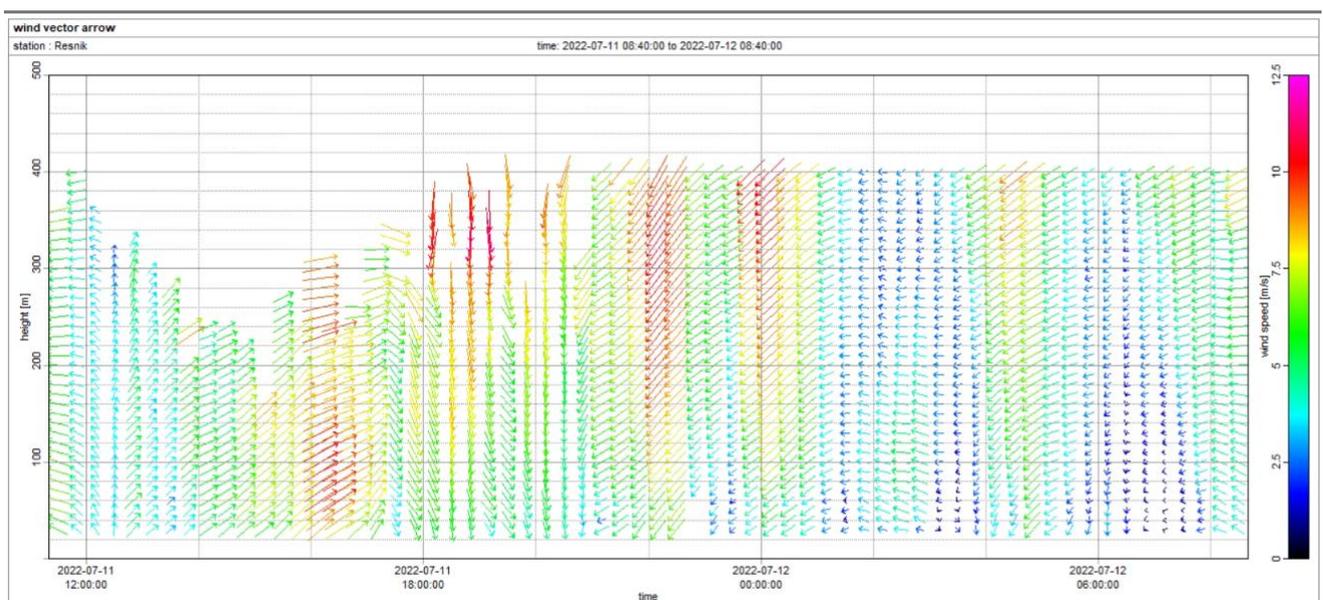
Figure 30 Wind profile for 11 July 2022. Plot was downloaded directly from MFAS SODAR APRun software.
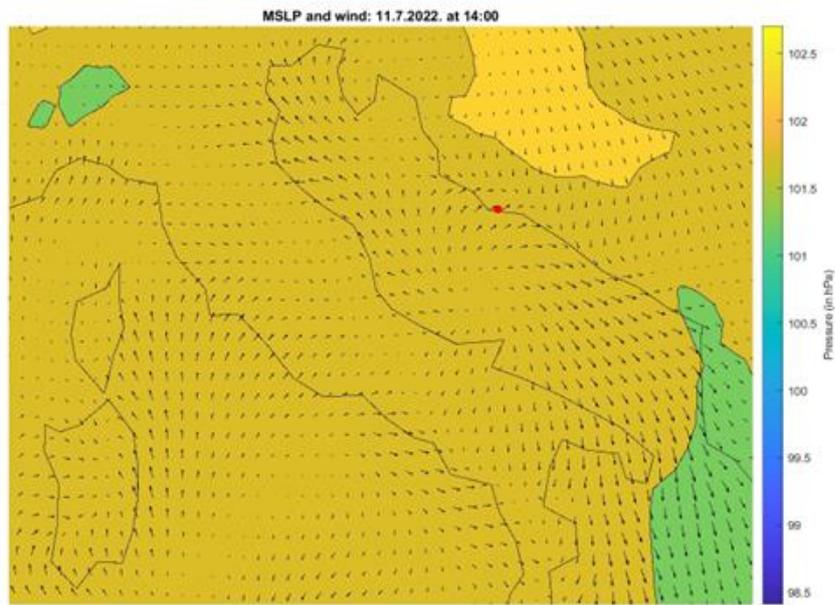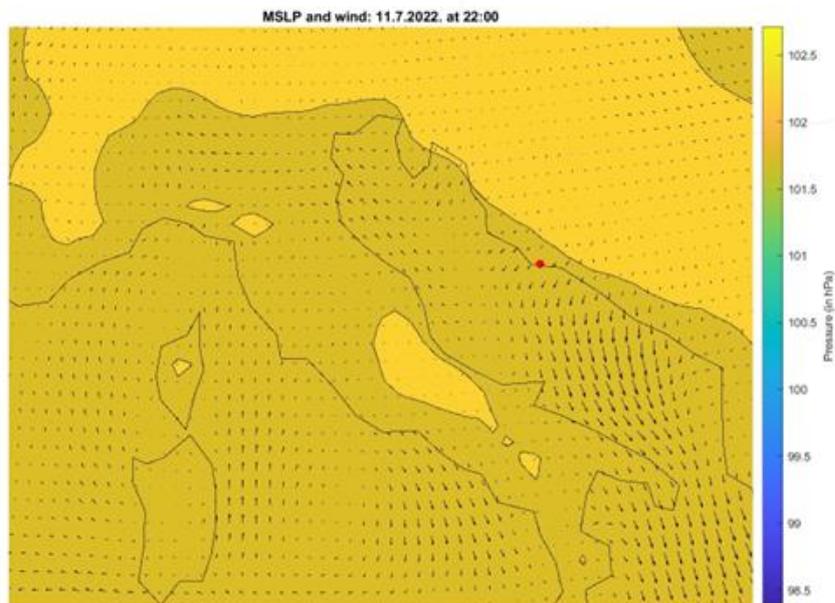
Figure 31 MSLP and wind field over the Adriatic Sea.

5.3 Episode without LSB 4 November 2022.

To specify a case without LSB circulation, we focus on 4.11.2022. when there was no LSB circulation (shown on Figure 32) In both moments (15:00 CET and 23:00 CET) the wind is firstly blowing in the direction of northwest and secondly blowing in the same direction as the low pressure field appeared (Figure 33a and Figure 33b).

The sea-breeze front can advance L = 10 to 200 km inland by the end of the day, although typical advances are L = 20 to 60 km unless inhibited by mountains or by opposing synoptic-scale winds. For the case of this research the Kozjak mountain represents a barrier of height of 779 m. Even without mountain barriers, the sea breeze will eventually turn away from its advance due to Coriolis force.
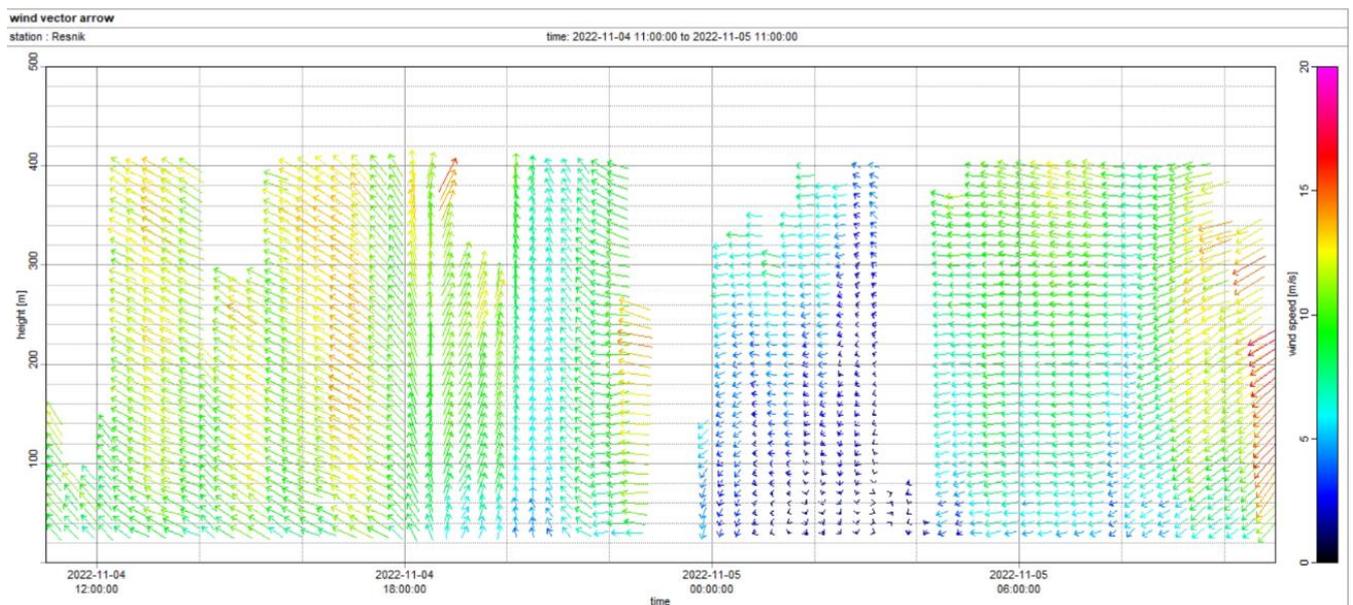
Figure 32 Wind profile for 4 November 2022. Plot was downloaded directly from MFAS SODAR APRun software.
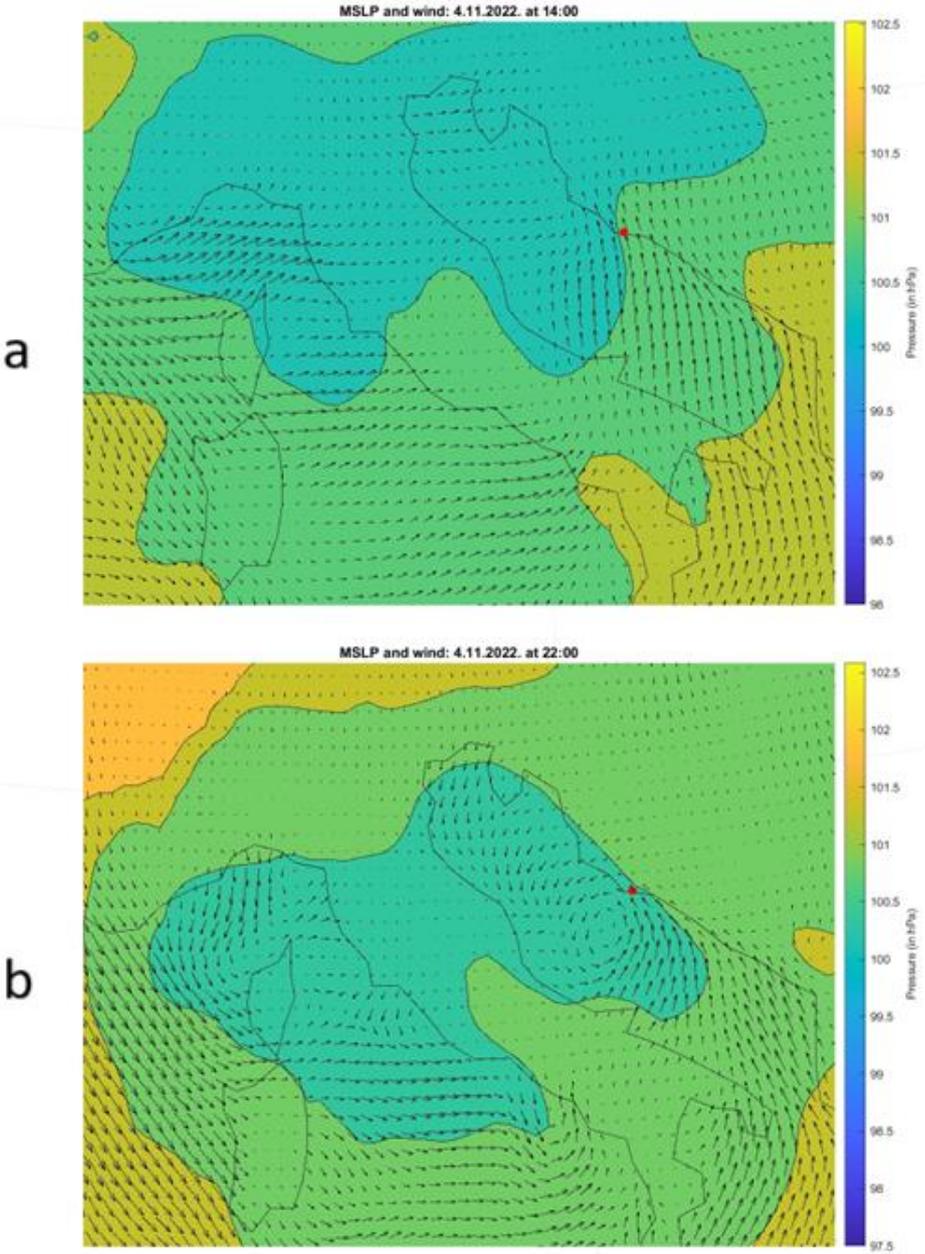
Figure 33 MSLP and wind field over the Adriatic Sea.

6 Conclusions

The Mediterranean Sea is geographically favorable for some specific local winds to occur. The Scintec Acoustic Wind Profiler SODAR MFAS data for June – November 2022 was analysed in this thesis. Of the available 164 days, we had 111 days for analysis, or more precisely 67.7%. Gap in the data set could have likely been caused by technical issues (device connected to laptop needed to be updated, low battery, bad weather, etc.). When increasing altitude there are fewer data set available (Figure 6), but what also needs to be pointed out is that during the summer there was lack of data from 200 m and higher altitudes at 13:20-17:20 (provided in Figure 7) just when the LSB circulation is the strongest.

By comparing June to August wind rose plots, I conclude that at ground level during the three months, dominant winds were southwesterly with speeds up to 10 m/s. At the altitude of 200 m, dominant winds were southwesterly during all three months, and northeasterly during July and August. At height of 400 m, dominant June winds were northerly (northwesterly to northeasterly) and dominant July and August winds were northeasterly. From Figure 12 we can notice that in all three months (September-October-November) the most frequent surface wind was southeasterly wind with speeds reaching up to 8-16 m/s. During October and November, northwesterly wind was also quite common. This is different from June to August when prevailing wind was southwesterly. At altitude of 200 m the prevailing winds were also southeasterly, again quite different than what was measured in June to August. At height of 400 m, dominant winds during September and October were southeasterly and northeasterly with speeds up to 7-9 m/s. In November, however, northwesterly winds were most frequent. Characteristic wind speeds reached up to 10-12 m/s. By examining the monthly wind roses, we can follow and study changes between the months and between summer and autumn season. From the theoretical background it is known that the velocity of the wind increases with height. [4]

By evaluating the mean sea level pressure (MSLP) and 500 hPa geopotential height as obtained from ERA5, I found out what kind of synoptic situations are suitable for occurrence of land and sea breeze in the area of the Adriatic Sea. To initiate a sea breeze circulation, it is essential for the synoptic scale pressure spatial gradient to be relatively weak. This is crucial because robust synoptic scale pressure gradients can dominate and hinder the development of sea breeze circulation. The significance of land-sea circulation is illustrated in the plots below, emphasizing factors such as pressure gradient, wind magnitude, and wind direction. Across the Croatia region, the average Mean Sea Level Pressure (MSLP) fields exhibit uniformity on days when sea breezes occur, lacking notable spatial gradients. Table 4 provides information on the frequency of days with and without land and sea breeze circulation during the investigation period. Specific events were examined too: having land and sea breeze (in Figure 31) and an episode of the sirocco wind (shown in Figure 32). The land and sea breeze can penetrate inland up to Kozjak mountain ~6km. The beginning of the LSB circulation starts with the summer season, and the sea breeze occurred at 15:00 CET till the land breeze started to cancel out at 23:00 CET. Northeasterly wind (sea breeze) started with velocity of 6 m/s and moved inland, till the southwesterly (land breeze) with smaller velocity ~4m/s started to cancel out. Land and sea breezes were dominant winds in this period, in particular during June to August.

In this research work it is shown that the Adriatic coast is quite favorable for circulation of land and see breeze wind. The analysis primarily focuses on pressure gradients, geopotential height, and wind patterns during sea breeze days compared to the entire month, providing insights into the atmospheric conditions influencing sea breeze events in the Mediterranean region. Due to given data set, the main focus was on land and sea breeze circulation, but if the data set was including whole year bora wind and sirocco could be examined into more detail too. Future works are needed to investigate and clarify these cases. This work of mine should be considered as preliminary result for the land and sea breeze circulations, due to the shortness of data set.

7 Literature

[1] URL: Flat Array SODAR MFAS (scintec.com)

[2] K. Zaninović, M. Gajić-Čapka, M. Perčec Tadić et al, (2008.) *Klimatski atlas Hrvatske /Climate atlas of Croatia 1961-1990., 1971-2000.* Državni hidrometeorološki zavod, Zagreb, 200 str.

[3] B.Ivancan-Picek, V.Tutis, V. Vukicevic, V. Vukicevic (1996). *Severe Adriatic jugo wind.* Meteorologische Zeitschrift. 5. 67-75.

[4] R. Stull, *Practical Meteorology: An Algebra-based Survey of Atmospheric Science.* UBC, 2015.

[5] S.A. Hsu., *Coastal Meteorology.* Academic Press, Inc. 1988.

[6] M.Telišmanj Prtenjak, *Main characteristics of sea/land breezes along the eastern coast of the Northern Adriatic*. (2003), Faculty of Science, Zagreb.

[7] URL: Sea-Breeze Circulations | BIP-MT Demonstration Module (psu.edu)

[8] H.Hersbach et al. *The ERA5 Globar Reanalysis* Quarterly Journal of the Royal Meteorological Society, 146, (2020), 1999-2049.

[9] Citing the data: Hersbach, H., Bell, B., Berrisford, P., Biavati, G., Horányi, A., Muñoz Sabater, J., Nicolas, J., Peubey, C., Radu, R., Rozum, I., Schepers, D., Simmons, A., Soci, C., Dee, D., Thépaut, J-N. (2023): ERA5 hourly data on pressure levels from 1940 to present. Copernicus Climate Change Service (C3S) Climate Data Store (CDS), DOI: 10.24381/cds.bd0915c6 (Accessed on DD-MMM-YYYY)

[10] V.Vukičević, V. Jurčec, B.Ivancan-Picek, *Adriatic jugo wind during 2000 - 2004.*(2005). 418-421.

[11] M.Orlic, B.Penzar, I. Penzar, *Adriatic Sea and Land Breezes: Clockwise Versus Anticlockwise Rotation*. Journal of Applied Meteorology. (1988.),27. 675-679. 10.1175/1520-0450(1988)027<0675:ASALBC>2.0.CO;2.

[12] B.Grisogono, D. Belusic, *A review of recent advances in understanding the meso-and microscale properties of the severe Bora wind*. (2009), 10.3402/tellusa.v61i1.15531.

A Appendix – Codes

A.1 Loading multiple files

```matlab
data = readtable('211228.txt', 'VariableNamingRule', 'preserve');
list=dir('C:\Users\38599\Desktop\Podaci\*.txt');
n=length(list);
        TIME=[];
        SPEED=[];
        DIR=[];
        W=[];
        SIGMAW=[];
        TIME1=[];
        HEIGHT=30:10:400;
        HEIGHT=HEIGHT';
        l=0;
 for k = 1:n
     name=list(k).name;
     data = readtable(name);
     data=rmmissing(data);
         if height(data)==2698
             date1=[2022,str2double(name(3:4)),str2double(name(5:6))];
             date2 =
datenum(date1)+1200/(60*60*24):datenum(0,0,0,0,0,1200):datenum(date1)+1-
1200/(60*60*24);
             date3 = datetime(date2,'ConvertFrom','datenum');
                 speed=data(:,2);
                 dire=data(:,3);
                 w=data(:,4);
                 sigw=data(:,5);
                         reshape_speed=reshape(speed{:,:}, [38,71]);
                         reshape_dire=reshape(dire{:,:}, [38,71]);
                         reshape_w=reshape(w{:,:}, [38,71]);
                         reshape_sigw=reshape(sigw{:,:}, [38,71]);
             SPEED=[SPEED,reshape_speed];
             SPEED(SPEED==99.9900)=[NaN];
             DIR=[DIR,reshape_dire];
             DIR(DIR == 999.900)=[NaN];
             W=[W,reshape_w];
             W(W == 99.9900)=[NaN];
             SIGMAW=[SIGMAW,reshape_sigw];
             SIGMAW(SIGMAW == 99.9900)=[NaN];
             TIME=[TIME,date3];
             TIME1=[TIME1,date2];

         else
             l=l+1;

         end
        end
```

A.2 Windrose plot

```matlab
%% June Windrose plot
    figure
    %subplot(4, 1, 1); set(gcf, 'units', 'normalized','position', [0 0 1 1]);
    Options8 = ['ndirections', 16, 'anglenorth', 0, 'angleeast', 90, {'axes',
subplot(4, 2, 1), 'cmap', 'jet'}];
    [ count8, speeds8, directions8, Table8] = WindRose(DIR(1,72:852),
SPEED(1,72:852), Options8); %za visinu 30
    title('Windrose(Lipanj): Height 30 m')
    subplot(4, 1, 2); set(gcf, 'units', 'normalized','position', [0 0 1 1]);
    Options1 = ['ndirections', 16, 'anglenorth', 0, 'angleeast', 90, {'axes',
subplot(4, 2, 2), 'cmap', 'jet'}];
    [ count1, speeds1, directions1, Table1] = WindRose(DIR(8,72:852),
SPEED(8,72:852), Options1);
    title('Windrose(Lipanj): Height 100 m')
    %WindRose(DIR(1:432,13),SPEED(1:432,13))  %150
    axes1 = subplot(4, 1, 3);
    Options2 = ['ndirections', 16, 'anglenorth', 0, 'angleeast', 90, {'axes',
subplot(4, 2, 3), 'cmap', 'jet'}];
    [ count2, speeds2, directions2, Table2] = WindRose(DIR(13,72:852),
SPEED(13,72:852), Options2);
    title('Windrose(Lipanj): Height 150 m')

    %WindRose(DIR(1:432,18),SPEED(1:432,18),'ndirections', 16, 'anglenorth',
90, 'angleeast', 180 )  %200
    Options3 = ['ndirections', 16, 'anglenorth', 0, 'angleeast', 90, {'axes',
subplot(4, 2, 4), 'cmap', 'jet'}];
    [ count3, speeds3, directions3, Table3] = WindRose(DIR(18,72:852),
SPEED(18,72:852), Options3);
    title('Windrose(Lipanj): Height 200 m')
    %WindRose(DIR(1:432,23),SPEED(1:432,23),'ndirections', 16, 'anglenorth',
90, 'angleeast', 180)  %250
    Options4 = ['ndirections', 16, 'anglenorth', 0, 'angleeast', 90, {'axes',
subplot(4, 2, 5), 'cmap', 'jet'}];
    [count4, speeds4, directions4, Table4] = WindRose(DIR(23,72:852),
SPEED(23,72:852), Options4);
    title('Windrose(Lipanj): Height 250 m')
    %WindRose(DIR(1:432,28),SPEED(1:432,28),'ndirections', 16, 'anglenorth',
90, 'angleeast', 180)  %300
    Options5 = ['ndirections', 16, 'anglenorth', 0, 'angleeast', 90, {'axes',
subplot(4, 2, 6), 'cmap', 'jet'}];
    [ count5, speeds5, directions5, Table5] = WindRose(DIR(28,72:852),
SPEED(28,72:852), Options5);
    title('Windrose(Lipanj): Height 300 m')
    %WindRose(DIR(1:432,33),SPEED(1:432,33),'ndirections', 16, 'anglenorth',
90, 'angleeast', 180)  %350
    Options6 = ['ndirections', 16, 'anglenorth', 0, 'angleeast', 90, {'axes',
subplot(4, 2, 7), 'cmap', 'jet'}];
    [ count6, speeds6, directions6, Table6] = WindRose(DIR(33,72:852),
SPEED(33,72:852), Options6);
    title('Windrose(Lipanj): Height 350 m')
    %WindRose(DIR(1:432,38),SPEED(1:432,38),'ndirections', 16, 'anglenorth',
90, 'angleeast', 180)  %400
    Options7 = ['ndirections', 16, 'anglenorth',0, 'angleeast', 90, {'axes',
subplot(4, 2, 8), 'cmap', 'jet'}];
    [ count7, speeds7, directions7, Table7] = WindRose(DIR(38,72:852),
SPEED(38,72:852), Options7);
    title('Windrose(Lipanj): Height 400 m')
```

A.3 ERA5 Reanalysis Code

```
info=ncinfo('500hPa19.11.22.nc');
lat=double(ncread('500hPa19.11.22.nc', 'latitude'));
long=double(ncread('500hPa19.11.22.nc', 'longitude'));
time=ncread('500hPa19.11.22.nc', 'time');
time=datetime(1900,1,1)+hours(time);
geopot=ncread('500hPa19.11.22.nc','z');
temp=ncread('500hPa19.11.22.nc','t');
u=ncread('500hPa19.11.22.nc', 'u');
v=ncread('500hPa19.11.22.nc','v');
info2=ncinfo('MSLP31.11.22.nc');
MSLP=ncread('MSLP31.11.22.nc', 'msl');
lat1=ncread('MSLP31.11.22.nc', 'latitude');
long1=ncread('MSLP31.11.22.nc', 'longitude');
time1=ncread('MSLP31.11.22.nc', 'time');
time1=datetime(1900,1,1)+hours(time1);
u1=ncread('MSLP31.11.22.nc', 'u10');
v1=ncread('MSLP31.11.22.nc','v10');

u500=u(:,:,1);
v500=v(:,:,1);
uMean=u1(:,:,1);
vMean=v1(:,:,1);
meanW500=sqrt(u(:,:,1).^2+v(:,:,1).^2);
Direc500=atand(u(:,:,1)./v(:,:,1));
meanMSLW=sqrt(uMean(:,:,1).^2+vMean(:,:,1).^2);
DirecMSL=atand(uMean(:,:,1)./vMean(:,:,1));
geopot = geopot(:,:,1);
sc=5;



[X,Y]=meshgrid(long,lat);
u500=u500';
v500=v500';
figure
load coastlines
worldmap('europe')
contourfm(Y,X,(geopot'/9.81), 'LineColor', 'w')
c=colorbar;
geoshow(coastlat,coastlon,'color','k')
hold on
xlabel ('Longitude [°]')
ylabel('Latitude [°]')
title('Geopotential and wind (at 500 hPa): 1.11.2022. 14:00')
hold on
c.Label.String = 'Geopotential (in m)';
geoshow( 43.5, 16.17, 'DisplayType', 'Point', 'Marker', 'o', 'Color', 'red',
'MarkerFaceColor','red');
quiverm(Y(1:sc:end,1:sc:end),X(1:sc:end,1:sc:end),v500(1:sc:end,1:sc:end),u500(
1:sc:end,1:sc:end),'k')
```